2004

Single phase thermohydraulic performance analysis of microchannel flow geometry for direct chip cooling

Harshal R. Upadhye

SINGLE PHASE THERMOHYDRAULIC PERFORMANCE ANALYSIS OF MICROCHANNEL FLOW GEOMETRY FOR DIRECT CHIP COOLING

By

Harshal R. Upadhye

A Thesis Submitted in Partial Fulfillment of the Requirement for the

MASTER OF SCIENCE
IN
MECHANICAL ENGINEERING

Approved by:

Dr. Satish G. Kandlikar
Department of Mechanical Engineering (Thesis Advisor)

Dr. Jeffrey D. Kozak
Department of Mechanical Engineering

Dr. Abhijit Mukherjee
Department of Mechanical Engineering

Dr. Edward C. Hensel
Department Head of Mechanical Engineering

DEPARTMENT OF MECHANICAL ENGINEERING
ROCHESTER INSTITUTE OF TECHNOLOGY

NOVEMBER, 2004

Single Phase Thermohydraulic Performance Analysis of Microchannel Flow Geometry for Direct Chip Cooling

Permission Granted

I, Harshal R. Upadhye, hereby grant permission to the Wallace Library of the Rochester Institute of Technology to reproduce my thesis in whole or in part. Any reproduction will not be for commercial use or profit.

Date: December 05, 2004 Signature of Author HR Upaghye

Acknowledgements

First of all I would like to thank my advisor Dr. Kandlikar for his continuous guidance, support and encouragement for this work. It has been a privilege to work with him in the lab. I would also like to thank everyone in the Thermal Analysis and Microfluidics Laboratory, especially Dr. Mukherjee and Mark for their help and insight.

I am also grateful to the Mechanical Engineering Department for opportunity to study and work here. I have had the best resources available for the last two years which definitely helped me in completing my thesis. I take this opportunity to thank Bill Finch for helping me with all software and hardware related issues.

Finally, I want to thank my family for their love, faith and sacrifice.

Abstract

One of the most important parameters affecting the performance of silicon integrated circuits is the junction temperature. Maintaining the junction temperature below a certain limit is very important for reliable operation. Most of the cooling for such circuits is done using air as a coolant. Current trends indicate that with improvement in the fabrication technology silicon chips with millions of devices are being fabricated. These trends point to very high heat fluxes in chip modules. To maintain the junction temperature of the circuits in such a scenario is a daunting task, and fabrication of such devices might be limited by cooling capability.

Direct Chip cooling with microchannels is a good solution for cooling of such devices. These chips have microchannels fabricated on the back side, through which cooling liquid such as water is pumped. The cooling water removes the heat from the chip. These microchannels can be fabricated along with the circuit components. Liquid cooling will also provide additional benefits of superior thermal properties.

The design and optimization of such systems are important from an operational standpoint. Pressure drop is an important parameter which governs the required pumping power and the pressure to which the chip is subjected. In present work, an optimization is carried out to identify the channel configuration that yields a minimum pressure drop for a given heat load. The constraints for the optimization are the maximum allowable chip temperature, the heat dissipated and the manufacturing constraints.

Table of Contents

List of Figures

List of Tables

Nomenclature

A_c	cross sectional area of fin, m^2
A_{div}	area offered by each division for heat transfer, m^2
A_s	surface area, m^2
A_w	area offered by the channel walls for heat transfer, m^2
a	channel width, m
b	channel depth, m
C_p	specific heat at constant pressure, kJ/kgK
D	diameter, m
d	hydraulic diameter of the channel, m
F	fin aspect ratio
f	friction factor
f_{app}	apparent friction factor
h	heat transfer coefficient, W/ m^2K
k	thermal conductivity of water, W/mK
K	constant in curve fitting equation, 4-37
k_f	thermal conductivity of fin material (silicon), W/mK
L	channel length , m
L_{hy}	hydraulic entry length, m
L_{th}	thermal entry length, m
m	fin efficiency constant defined by Eq. 6
$\dot{m}_c$	mass flow rate through single channel, kg/s
N	number of divisions
n	number of channels that can be fitted in heat sink
Nu	Nusselt number
$N_{\Delta p}$	pressure difference number
N_{work}	work rate number
P	perimeter of channel, m
Pr	Prandtl number

Q	heat rate, W
Q_{div}	heat dissipated per division, W
q''	heat flux, W/ m^2
q_{max}	maximum heat dissipated by fin, W
q_f	heat dissipated by fin, W
Re	Reynolds number
s	thickness of the fin, m
T_b	Fluid bulk temperature, K
T_{fin}	fin temperature as a function of fin length and height, K
T_{out}	temperature at the outlet of the microchannels, K
T_{in}	temperature at inlet of the microchannels, K
T_s	surface temperature of the heat sink, K
V	fluid velocity through the microchannel, m/s
W	width of the chip to be cooled, m
$\dot{w}$	pumping power, W
X	x-axis variable in curve fitting
x	axial distance from the entrance of the channel, m
x^+	hydrodynamic entry length
x^*	thermal entry length
Y	y-axis variable in curve fitting

Greek Symbols

α	channel aspect ratio
β	ratio of fin thickness to channel depth
η_f	fin efficiency
ρ	density, kg/ m^3
μ	dynamic viscosity, Ns/ m^2
ν	kinematic viscosity, m^2/s
υ	volume in m^3
Δp	pressure drop, Pa

ΔT temperature difference, K

Θ_b temperature difference at the base of fin, K

θ thermal resistance, ^{0}C/W

θ_{cond} conduction resistance, ^{0}C/W

θ_{conv} convective resistance, ^{0}C/W

θ_{heat} resistance due to heating of fluid, ^{0}C/W

Chapter 1: Introduction

Thermal management of electronic devices is one of the important aspects for electronics packaging. Air has been a preferred choice for cooling such electronics packages. With the rapid advances in microelectronics technology, the volume occupied by the devices has reduced considerably due to reduction in the feature size. But with an increasing demand for faster and more efficient circuits, the power dissipation and number of circuits per unit volume has increased. The combined effect of this is an increase in the junction temperature. The increased temperature affects electrical performance of the device and reduces its reliability. Manufacturers of electronics devices estimate that for every 10°C rise in the junction temperature, the device failure rate is doubled. A very high operating temperature might damage the electronic circuitry to a point of complete failure. Possible damage involves junction fatigue, changes in electrical parameters and a thermal runaway condition.

The famous forecast by Intel founder Gordon Moore, who in the late 1960s predicted the number of transistors on a chip would roughly double every two years, known as the "Moore's Law," has held true since then. In 1992, a 486/DX2 66Mhz CPU consumed about 7W of power (with 1.2 million transistors). It didn't even require a cooling fan. In 2003, the new Itanium II uses up to 130 W (with 220 million transistors). Contradicting fears that the semiconductor industry's pace of development is slowing, Intel Corporation announced in August 2004 that it has achieved a milestone in shrinking the size of transistors that will power its next-generation chips. The company created a fully functional 70 megabit memory chip with each transistor switch measuring just 35 nanometers. As a result of this reduction in size, more of these tiny devices can be squeezed onto a single chip. By 2005 Intel is due to release processors in the range of 6 GHz and the method of cooling for these chips is still unknown. The power consumption of a typical Intel CPU is shown in fig 1-1.

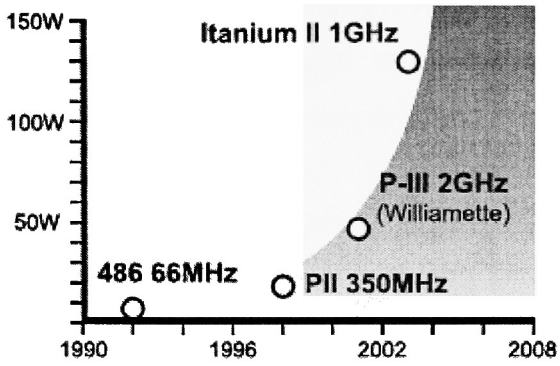

Figure 1-1: CPU Maximum Power Consumption.

Heat removal from electronic circuits has been a research topic for many years and a number of new technologies have been considered. Initially, air was the preferred fluid for cooling electronic packages. It is still a preferred method for cooling devices which do not dissipate large power. Cooling with air has inherent advantages, like simple cooling system, low cost, ease of maintenance and high reliability. Figure 1-2 shows a typical fan and heat sink arrangement. Extensive research has already done on air cooling of electronics devices and considerable knowledge has been gained. Air cooling relies on various heat transfer enhancement techniques. Finned heat sinks, which increase surface area for convection, are very common on electronics devices.

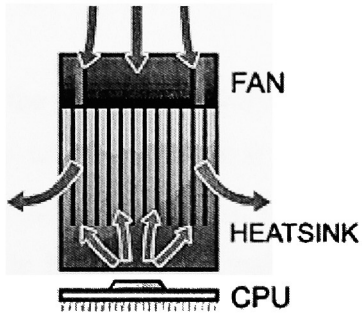

Figure 1-2: Heat Flow in a Typical Fan and Heat Sink arrangement.

These heat sinks are attached to the electronic component and fans are utilized to force air to flow over the fins. However, air has low thermal conductivity and Prandtl

number. Density and specific heat of air are not high. As a result, air cannot carry a large amount of thermal energy without experiencing a very high temperature rise. The heat transfer from the fins to the cooling medium, air in this case, depends upon the thermal resistance between the two. The convective thermal resistance is very large when utilizing air cooling. Therefore, to remove a certain amount of heat from a chip, the temperature difference between the fins and the air flowing over them must be large. This results in a very high circuit temperature, which is unacceptable. Other disadvantages associated with are cooling are high noise level and pressure drops for heat sinks employing large air flow rates. Heat pipe is the most commonly employed cooling device in portable computers. Heat pipes have the advantage of not consuming any external power. The working fluid is contained in a closed chamber. The heat pipe transports heat from the high powered chip to a suitable area where it can be spread using a metal plate. These capillary driven heat pipes are not suitable for high heat flux applications because of the increase in the size of the heat pipe.

Liquid cooling, which uses liquid instead of air, is gaining considerable attention as an alternative in the high heat flux cooling applications. Nakayama (1999), in his review paper focused on removal of large amounts of heat from a very small physical space. He considered cooling techniques like low velocity air cooling, heat sinks using low speed air flow, heat sinks with high speed air impingement, direct single-phase cooling, phase change cooling and heat pipes.

Physical properties of the coolant are very important while designing a cooling system. Thermal conductivity and specific heat are two important properties to be considered. Thermal conductivity is the amount of energy that can be carried away by the material per unit time. Table 1.1 shows thermal conductivity values in W/mK.

Material	Thermal Conductivity (W/mK)
Copper	393.7
Silicon	150
Water	0.67
Air	0.026

Table 1-1: Thermal Conductivities of various materials.

Specific heat is the amount of heat stored in a particular material. The specific heat gives us an idea as to how many kilojoules of energy will be required to change the temperature of unit mass of material by one Kelvin. Table 1-2 gives values in kJ/kgK

Material	Specific Heat (kJ/kgK)
Copper	0.39
Silicon	0.7
Water	4.184
Air	1

Table 1-2: Specific heat values for various materials.

The thermal conductivity of copper is very high and hence is a very good material for conducting away heat. Water has very good thermal properties and can be used to remove heat away effectively. In an ideal situation we can use copper to carry heat away from the hot processor and then use water to remove it to some other location where it can be rejected to the atmosphere.

Direct chip cooling with the help of microchannels or minichannels offers a practical solution to the problem of ever-increasing heat dissipation requirements of such chips. In such a system, the chip will have the channels fabricated on it through which cooling fluid such as water will flow. The design and optimization of such a system is important from an operational standpoint. Pressure drop is an important parameter which dictates the pumping power required and the pressure to which the chip is subjected. Channel width, depth and the fin thickness influence the performance of the heat sink and hence should be selected properly. An optimization is carried out to identify the channel configuration that yields a minimum pressure drop for the given heat load. The constraints for the optimization will be the maximum allowable chip temperature, the heat dissipated and manufacturing constraints which will allow only certain configurations.

The concept of direct chip cooling using single phase heat transfer was first given by D.B. Tuckerman and R.F.W. Pease (1981). In this pioneering work they showed that finned heat exchangers with small flow channels are capable of dissipating large amount of energy. In their work, heat exchangers with microscopic dimensions were built and were expected to cool circuits with power densities more than 1000W/cm^2. The thermal resistance of a heat sink is defined as

$$\theta = \frac{\Delta T}{Q} \tag{2-1}$$

where ΔT is the temperature rise of the circuit over the coolant inlet temperature and Q is the total dissipated power. The thermal resistance θ should be as small as possible to dissipate maximum energy without raising the circuit temperature above a prescribed upper limit. Tuckerman and Pease considered the thermal resistance to be made up of three components: θ_{cond} - conduction resistance through the heat sink thickness, θ_{conv} the convective resistance from the heat sink to the cooling fluid, and θ_{heat} -which is the heating resistance as the cooling fluid gets heated up. The two components θ_{cond} and θ_{heat} were neglected because they can be reduced by changing the substrate and cooling fluid. θ_{conv} was considered to be a major contributor to the thermal resistance and hence efforts were channeled towards reducing the θ_{conv}. θ_{conv} depends on the convective heat transfer coefficient h between channel wall and the fluid. Larger the value of h lower is θ_{conv}. The value of h is given by

$$h = \frac{Nuk}{d} \tag{2-2}$$

where k is thermal conductivity of the fluid, d is the characteristic length and Nu is Nusselt number. Nusselt number for a channel, depends on the shape of the channel cross section, varies between 3 and 9. With a constant value of the Nusselt number for laminar flows, d becomes the controlling parameter in predicting the heat transfer coefficient. Smaller the channel size, larger the value of h, and lower the convective resistance. To obtain higher h values, Tuckerman and Pease manufactured channels of microscopic dimensions. The walls separating the channels were analyzed as small fins. To account for the temperature distribution in the fins, they incorporated the fin efficiency in their analytical model. Their analysis was based on the assumptions that the flow was fully developed and laminar. The fin efficiency was fixed at 0.76 and the heat transfer from the bottom and top of the channel was neglected. For a heat sink of 1cm × 1cm substrate and a pressure drop of 30 psi, they calculated the thermal resistance to be $0.086^0 C/W$. Using the parameters obtained from the calculations, three high-performance heat sinks were fabricated, and a series of experiments were conducted. One device absorbed a heat flux of 790 W/cm^2 with a maximum substrate temperature rise of $71^0 C$ above the inlet water temperature.

Phillips, R.J., (1987) in his thesis 'Forced Convection, Liquid-Cooled, Microchannel Heat Sinks' extended the work done by Tuckerman and Pease (1981). The work done by Tuckerman and Pease was restricted to laminar flow. Phillips extended the theoretical analysis to include small, moderate, and large aspect ratio channels, for fully-developed and developing flow in the laminar and turbulent regimes. His analysis included the effects of variable properties of the chip material and that of the liquid coolant. Compressibility effects for the cooling liquid were found to be negligible. For maintaining the surface temperature uniformity on the chip, he introduced a concept called compensation heater, which reduces the thermal gradients around the integrated circuit. He classified the duct aspect ratio (the ratio of channel depth to channel width) in three categories. Aspect ratio greater than 10 are classified as large aspect ratio channels, aspect ratio between 1 and 10 are moderate aspect ratio channels and channels having a aspect ration less than 1 were small aspect ratio channels. The thermal resistance models for each case were different. The large aspect ratio channels have large fin heights. The

surface area available for heat transfer at the base of the channel is very small. Hence the convective resistance from the base of the channel was neglected in the proposed model. In case of the moderate aspect ratio channels the heat transfer from the channel base had to be considered. For the small aspect ratio channels the fins used are just for structural purposes. The fin height and fin width are small and do not contribute to heat transfer significantly. Therefore the thermal resistance due to the fins and the resistance due to constriction effect were neglected. The worst case thermal performance was predicted to occur at the exit of the microchannel. Hence the thermal performance was predicted at the exit, for a more conservative approach. The unknown in his formulation was the coolant velocity through the channel. Three types of design constraints – fixed pressure drop through the heat sink, fixed volumetric flow rate per unit heater surface area and fixed pumping power per unit heater surface area were used to obtain the coolant velocity. Once the coolant velocity was known, the heat transfer coefficient was obtained from the Nusselt number.

The total thermal resistance is obtained by substituting the values of the coolant velocity and the heat transfer coefficient into various thermal models. He wrote a computer program MICROHEX to compute the thermal and fluid flow performance for forced-convection, liquid-cooled, microchannel heat sinks. The models for large, moderate and small aspect ratio channels were included in the program to handle developing and fully developed flow in both laminar and turbulent regimes. He concluded that the overall thermal resistance is dominated by the convective and capacitance terms. Developing flow gave a better performance, and in case of wide channels, turbulent flow was found to be better than laminar flow.

Samalam, V.K., (1989) presented an analytical solution to find optimum dimensions for the channel width and spacing in a microchannel heat exchanger. He simplified the problem of convective heat transfer in microchannels. The problem was reduced to a nonlinear differential equation and an exact solution was obtained. The solution is in the form of fin temperature along the length and the height of the fin (T_{fin} is a function of length and height of the fin). The maximum fin temperature was found to

be at the base of the fin (height = 0) at the exit. He concluded that for a good performance, the aspect ratio of the channel should be as large as possible. He further added that taking into consideration manufacturing constraints, an aspect ratio between 4 to 6 represents a good solution.

Riddle *et al.* (1991) in their paper compared the results obtained from their computer code MCHSCALC to the experimental results. Two different aspect ratio channels were tested – 9:1 and 17:1. The 9:1 channel ratio was the optimum ratio for water cooling according to their calculations. The 17:1 was the fabrication limit for the dicing saw they used. Two types of 9:1 ratio silicon microchannel heat sinks were tested. In one of the heat sinks, a thin tungsten carbide resistive film was sputtered onto the top of the heat sink. This was to simulate direct bonding of an active device to the microchannel heat sink. Another heat sink was fabricated with a piece of silicon bonded to the microchannel heat sink and the resistive film applied to the silicon piece. The channel dimensions used were $51\mu m$ wide and $445\mu m$ deep for the 9:1 aspect ratio channel and the same width with a depth of $825\mu m$ for the 17:1 aspect ratio channel. The 17:1 aspect ratio had resistors attached to its surface to simulate heating.

The MCHSCALC code was based on the analysis performed by Tuckerman and Pease. In their experimental work, thermal resistance was measured using thermal imaging camera to measure the temperature rise of the heated surface. Comparison between the values obtained from MCHSCALC and the experimental data obtained were done for the case with 100W power input. The predicted resistance for $100W/cm^2$ power input was $0.115cm^2\,^0C$ and experimental value was $0.093cm^2\,^0C$. The over prediction of the thermal resistance was attributed to the conservative method used to calculate the caloric thermal resistance. The thermal resistance remained constant in their experiments within the limits of experiments. They reported that the experimentally measured thermal resistance is nearly independent of the power level over a significant range, $100W/cm^2$ to $2500W/cm^2$.

Knight *et al.* (1992) presented a scheme for optimizing the microchannel heat sinks. The thermal conductivity of the material used for the heat sink, the overall dimensions of the heat sink, coolant properties, maximum allowable pressure drop or pumping power and the fin efficiency were assumed to be known. The model analyzed the flow in heat sink as a two-dimensional flow through very small rectangular channels having a constant wall heat flux boundary condition. The heat sink was supposed to have n number of channels and n-1 fins. In their work the problem was generalized using dimensionless variables. The dimensionless thermal resistance was defined as the thermal resistance (as given in Eq 2-1) multiplied by the thermal conductivity of the fluid and the width of the heat sink. Two more dimensionless parameters, pressure difference number, $N_{\Delta p}$ and work rate number, N_{work} are defined. The pressure difference number is defined as

$$N_{\Delta p} = \frac{\left[\frac{\Delta p}{L}\right] W^3}{\rho \nu^2} \tag{2-3}$$

where L is the length of the heat sink in the direction of the flow and W is width of the heat sink. Work rate number is given by

$$N_{work} = \frac{\dot{w} W}{\rho \nu^3} \tag{2-4}$$

Other dimensionless groups defined were thermal conductivity ratio k/k_f ; ratio of fin width to channel width s/a ; aspect ratio $\alpha = b/a$; the heat sink length to width ratio L/W and heat sink depth to width ratio d/W . Knight *et al.* (1991) in an analytical treatment of the design of forced convection heat sinks found that the design of such heat sinks should be constrained by maximum power consumption and not by allowable pressure drop. They showed that if the design is constrained by maximum pressure drop, the pumping power required for obtaining a minimum thermal resistance is comparable in magnitude to the amount of heat dissipated in the heat sink. An entire procedure for finding out the

thermal resistance is given in the paper. Both laminar flow and turbulent flow cases were considered. Their new optimization method was used to obtain various designs, and the results were compared with the work done by other researchers. A significant reduction in the thermal resistance was observed by changing the fin thickness to channel width ratio and resizing the channels. They concluded that when the flow is turbulent the thermal resistance is much less than the thermal resistance when the flow is laminar.

Choquette *et al.* (1996) presented a code for optimization of microchannel heat sink. The program uses the thermal resistance model and operated in two modes. An existing heat sink is analyzed in mode one and mode two is used as a design tool to optimize the heat sink. Apart from the analytical model presented, a finite difference numerical technique was used to solve the conjugate heat transfer problem. A comparison between the two is also made. The results were presented as a three dimensional plot of the heat sink thermal resistance as a function of fin thickness and channel aspect ratio. After analyzing both laminar and turbulent flow conditions they concluded that significant improvement over the laminar performance could not be achieved in the turbulent region when all the flow geometries were considered.

Zhimin and Fah (1997) set up a thermal resistance model to analyze the performance of a microchannel heat sink. Laminar, turbulent, developed and developing flow were considered in the analysis. Effects of heat sinks channel aspect ratio, fin width to channel width ratio and the channel width on the total thermal resistance is studied. Constant volumetric flow rate, constant pressure drop and constant pumping power conditions were analyzed. Analysis was done over a wide range of flow conditions and heat transfer regimes and the effects on flow rate, pressure drop and pumping power were investigated thoroughly. They concluded that the fin width to channel width ratio should be in between 0.5 and 0.65 to achieve a low thermal resistance. The channel aspect ratio should be set as high as possible to reduce the total thermal resistance. The turbulent flow yielded a lesser thermal resistance as expected but the pressure drop was very high.

Sobhan and Garimella (2001) compiled and analyzed results for heat transfer and fluid flow investigated by various researchers. A comprehensive review of investigations on microchannels is presented in the paper. Comparative study of correlations for friction factor and heat transfer is also presented. They compared correlations and results of investigations in flow and heat transfer in microchannels to conventional correlations for larger channels, tubes in laminar and turbulent regime. They concluded that the continuum assumptions were not violated for all the channels tested by the researchers which mostly had hydraulic diameters greater than 50μm. As a result analysis based on Navier-Stokes and energy equations were expected to correctly model flow and heat transfer through microchannels. The discrepancies in predictions might be due to the entry and exit effects, surface roughness in channels and nonuniformities in channel dimensions. They found considerable diversity in the results presented in the literature and concluded that reliable prediction of heat transfer rates and pressure drop in microchannels is a difficult task.

Qu and Mudawar (2002) tested microchannel heat sink 1cm wide and 4.8cm long. The microchannels machined in the heat sink were 231μm wide and 712μm deep. Apart from this they also presented numerical analysis for a unit cell containing a single microchannel and surrounding solid. The measured pressure drop across the channels and temperature distribution showed good agreement with the numerical results. They concluded that the conventional Navier-Stokes and energy equations remain valid for predicting fluid flow and heat transfer characteristics in microchannels.

Bergles *et al.* (2003) in their paper discussed boiling and evaporation in small diameter channel. Heat exchangers made with small channel dimensions have two basic problems – flow distribution in small channels parallel to each other and conjugate heat transfer effect. They studied both single phase and two phase heat exchangers in there paper. The paper considered the general design trade-offs in small-diameter channels. A general design problem was considered in which the heat rate Q (W) and the overall dimensions for the heat exchanger given. All other parameters like the channel dimensions, cooling fluid, number of channels are to be decided. The important factors

affecting the selection being the pressure drop and the pumping power required. General design guidelines were suggested and an example of channel size reduction was presented. The pumping power depends upon pressure drop through the channels which is an area under investigation. Pressure drop through microchannels is discussed later in this section.

Upadhye and Kandlikar (2004) presented analysis for optimizing the microchannel geometry for direct chip cooling using single phase heat transfer. A chip 25.4mm X 25.4mm was analyzed. A fully developed laminar flow with constant channel wall temperature and constant heat flux condition were considered. The analysis showed that from heat transfer and pressure drop perspectives, a narrow and deep channel is better than having a wide and shallow channel. For the chip size considered and a heat load of $100W/cm^2$ channel width between $150\mu m$ and $250\mu m$ gives optimum pressure drop with channel depth of $250\mu m$.

Steinke and Kandlikar (2004) carried out an extensive review of conventional single phase heat transfer enhancement techniques. Several passive and active enhancement techniques for conventional, Minichannels and microchannels are discussed at length. Some of the enhancement techniques discussed are fluid additives, secondary flows, vibrations and flow pulsation.

Suresh Garimella and Vishal Singhal (2004), in their work focused on fluid flow, heat transfer and pumping considerations in microchannel heat sinks. They observed a disparity in the data presented for pressure drop and heat transfer in microchannels. Hence they conducted fluid flow and heat transfer experiments on channels with hydraulic diameters in range of $250\mu m$ to $1000\mu m$. The results they obtained were compared to predictions from conventional correlations. In the experiments channels with various hydraulic diameters were fabricated and tested. For the fluid flow experiments, two approaches were used. Short microchannels with pressure taps beyond the length of microchannel and long microchannels with pressure taps along the length such that there is no effect of entrance or exit regions. The entrance and exit pressure

losses were calculated and subtracted from the measured values for the short channels. The results obtained from these experiments indicated that around Re= 2000 the laminar predictions for friction factors deviate from the experimental values indicating onset of turbulence. Flow visualization experiments were also carried out. The behavior of a dye streak injected in the flow was studied. If the dye streak maintained its integrity the flow was classified as laminar. Slight diffusion or blurring of the dye streak was considered as the onset of turbulent flow and once the channel cross section is completely filled with dye the flow was classified as turbulent. The visualization agreed with the pressure drop measurements and showed that the flow is laminar up to Re = 2000.

For heat transfer experiments a similar setup was used with some changes to measure temperature. The results were reported in terms of the Nusselt number. Results were reported for simultaneously developing flow, thermally developing laminar flow and turbulent flow. For low Reynolds number the experimental results matched the predictions for thermally developing laminar flows. As the Reynolds number increases the experimental results deviate from the laminar results. As the Reynolds number increases further the predicted Nusselt numbers are off by a large margin. After trying out several hydraulic diameters for channels, they concluded that below 1.2 mm channel diameter standard Nusselt number correlations are not useful.

Pumping techniques is an important aspect in microchannel cooling technology. Garimella and Singhal, presented a comprehensive review of micropumping technology. The review presented micropumping devices and their various parameters like size, operating voltage, power required per unit flow rate etc. They concluded that valveless, piezoelectric and electroosmotic micropumps are better suited for electronic cooling.

Sung Jin Kim (2004) in his paper titled 'Methods for Thermal Optimization of Microchannel Heat Sinks' focused on various design methodologies that led to optimum dimensions for a microchannel heat sink. The paper presented three optimization methods aimed at reducing the thermal resistance of microchannel heat sinks. The models presented where the fin model, the porous medium model and the numerical

optimization method. The simplest of all models, the fin model is popular than the others. The analysis done in the paper defines the thermal resistance as defined in equation 2-1. The flow is assumed to be thermally fully developed and the entire analysis is done the way Knight *et al.* (1991, 92) had done in their work. The effect of developing flow can be taken into account by using correlations developed for Nusselt number. The porous medium model considers the microchannel heat sink as porous medium saturated with the cooling fluid. The flow is assumed to be hydrodynamically and thermally full developed. In the numerical optimization method the energy equation is solved numerically. The numerical procedure is explained in detail by Ryu *et al.* (2001). Results from analytical models with porosity of 0.5 and a conductivity ratio of 0.005 were compared with the results from numerical model. The porous medium model predicted temperature distribution within 4% of the numerical solution. The results from the fin model varied depending on the aspect ratio of the channels. The comparison between the fin model and numerical model with varying thermal conductivity ratios showed a significant deviation between the solid temperature distributions. It was observed that the porous medium model predicted results in close agreement with the numerical solution results. The difference between results from fin model and the numerical model increase as the conductivity ratio and the aspect ratio increases.

Apart from the temperature distribution in the solid itself, the thermal resistance values obtained from these three models were compared. The thermal resistance predicted by the fin model was in close agreement with the numerical results when the aspect ratio was less than 8, but for aspect ratio greater than 8 significant deviations was observed. But with the porous medium model, the results match perfectly for any aspect ratio. Explanation as to why these discrepancies occur is also discussed in the paper. The fin model and the porous medium model both assume unidirectional conduction along the fin height. If conduction in the fluid flow direction is neglected in the numerical solution, the error due to assumption of one dimensional conduction is just 4%. The assumption of one-dimensional conduction is valid as long as the Biot number is less than 0.1. Assuming the heat transfer coefficient to be constant in case of fin model can introduce errors. The average value of heat transfer over the entire periphery of the

channel assumes that the difference between the heat transfer coefficient along the fin height and the channel base is small. As the channel aspect ratio increases the difference between two values increases which introduces errors. The fin efficiency used in the fin model assumes that the heat transfer coefficient is constant.

Chapter 3: Objectives of Present Work

This work presents the heat transfer and pressure drop analyses and the results of a heat sink performance employing microchannels directly on the back-side of a chip. The channel dimensions in case of direct chip cooling are important parameters that decide the thermal and hydraulic performance. An analytical procedure is developed for analyzing both fully developed and developing flow conditions. An algorithm is developed to obtain an optimum geometry that provides the lowest pressure drop for a given heat load by varying the channel width, the water mass flow rate and the fin thickness. Further investigation is carried out to develop channel configurations which yield the lowest pressure drop. The analysis is extended to an offset strip-fin configuration in which the heat transfer coefficient is calculated by using the developing flow equations. Another configuration of a split pass arrangement is also analyzed.

4.1: Introduction

Figure 4-1 shows microchannels fabricated on one side of an IC chip. The heat dissipating devices are on the bottom side of the structure. The length of the channels L and the width W are fixed by the chip geometry. The channel width a, the wall thickness between two channels s, and the channel depth b, are the main parameters of interest. The microchannels are machined or etched in the silicon substrate and are enclosed with a cover plate on the top to form the flow channels.

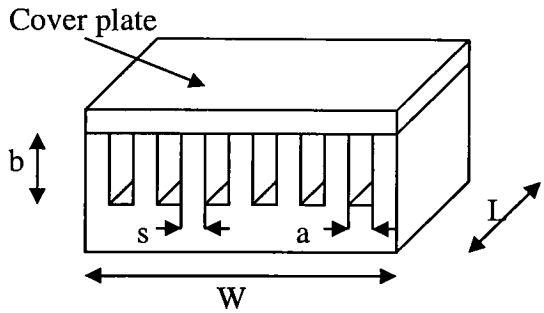

Figure 4-1 Microchannels Machined in Silicon

4.2: Channel Hydraulic Diameter

As the channel hydraulic diameter decreases, the ratio of the heat transfer surface area to the fluid flow volume increases in an inverse proportion to the channel hydraulic diameter. For example, in a circular channel this ratio is given by

$$\frac{A_S}{v} = \frac{\pi DL}{\left(\frac{\pi}{4}D^2 L\right)} = \frac{4}{D} \tag{4.1}$$

where A_s is the surface area, v is the volume and D is channel diameter. For a rectangular channel, the channel hydraulic diameter d is given by

$$d = \frac{4ab}{2(a+b)} \tag{4.2}$$

In the case of a laminar single-phase flow, with a constant Nusselt number, the heat transfer coefficient depends on the channel dimensions. The Nusselt number for laminar single-phase flow is given by

$$Nu = \frac{hd}{k} = \text{constant} \tag{4.3}$$

Rearranging the equation

$$h = \frac{Nuk}{d} \tag{4.4}$$

As the channel dimensions become small, the heat transfer coefficient increases as seen from Eq. (4.4). The heat transfer rate per unit flow volume is given by

$$\frac{q}{v} = \frac{hA_S\Delta T}{v} \tag{4.5}$$

Substituting equation 4.1 and 4.4 in equation 4.5 we obtain

$$\frac{q}{v} = \frac{hA_S\Delta T}{v} = Nu\frac{4k}{d^2}\Delta T \tag{4.6}$$

For a given fluid and a specified temperature difference, the volumetric heat transfer rate depends inversely on the square of channel diameter. But with the small channels the

pressure drop increases significantly. As a result, the flow rates employed in these systems are very low. The low flow rates associated with small channel dimensions result in laminar flows. The entire analysis in this section is carried out assuming a laminar flow.

4.3: Geometrical Parameters

The active surface area of the chip is defined by the length L and the width W. The channels are fabricated along the width of the active surface area. The separating wall in between the two adjacent channels is analyzed as a fin. So the total number of fins will be one more than the number of channels 'n'. For a given number of channels, the channel width is

$$a = \frac{W}{n + (n+1)F} \tag{4.7}$$

where fin aspect ratio, F is defined as the ratio of the fin thickness to the channel width.

$$F = \frac{s}{a} \tag{4.8}$$

The channel aspect ratio α, is the ratio of the channel width to the channel depth and is given by α. $0 < \alpha \leq 1$

$$\alpha = \frac{a}{b} \tag{4.9}$$

The aspect ratio of the channel is important because the friction factor and the Nusselt number are both dependent on the aspect ratio of the channel. β is defined as the ratio of fin thickness s to the fin length (which is also equal to the channel depth) b.

$$\beta = \frac{b}{s} \tag{4.10}$$

4.4: Fin Efficiency

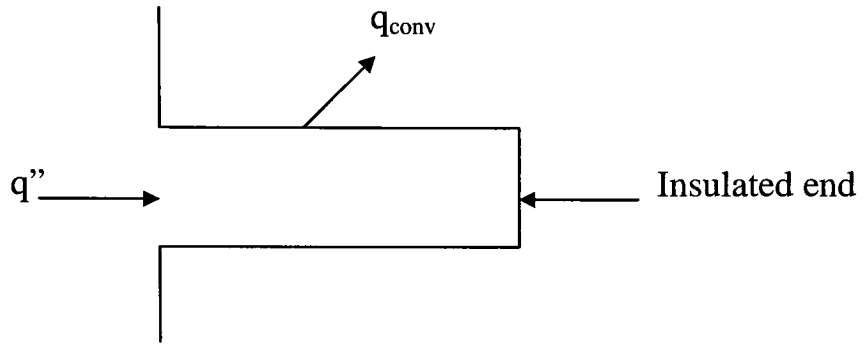

Figure 4-2: Fin of uniform cross section

The walls between two adjacent microchannels are treated as fins. Fins are considered as extended surfaces involving heat transfer within the solid by conduction and heat transfer by convection from the boundaries. The temperature difference between the fin base and the fluid is the driving potential for convection. If the entire fin is at the base temperature then the fin will dissipate energy at the maximum rate. But since the fin has a finite thermal conductivity, the temperature of the fin is not constant. The temperature is highest at the base and goes on decreasing as we go away from the base.

A measure of fin thermal performance is provided by the fin efficiency. Fin efficiency is defined as

$$\eta_f \equiv \frac{q_f}{q_{\max}} \tag{4.11}$$

where η_f is the fin efficiency, q_f is the heat dissipated by the fin and q_{max} is the maximum heat that can be dissipated. Assuming no convective heat loss from the fin tip, the heat transfer rate from the fin is

$$q_f = \sqrt{hPk_f A_c}\,\Theta_b \tanh mb \tag{4.12}$$

Where m is defined as

$$m = \sqrt{\frac{hP}{k_f A_c}} \tag{4.13}$$

In the Eq.4.13 P is the fin perimeter, A_c is the cross sectional area of the fin. Excess temperature at the base, Θ_b is defined as the temperature difference between the bulk temperature of the fluid and the temperature at the base of the fin. The maximum heat that can be dissipated, q_{max} is defined as

$$q_{max} = hA_f\Theta_b \tag{4.14}$$

Substituting Eq. 4.12 and Eq. 4.14 in Eq. 4.11 the equation for fin efficiency becomes

$$\eta_f = \frac{\tanh mb}{mb} \tag{4.15}$$

The perimeter of the fin is

$$P = 2(L+s) \tag{4.16}$$

The fin thickness is very small as compared to the channel length and hence the perimeter can be assumed to be twice the channel length.

$$P = 2L \tag{4.17}$$

The cross sectional area of the fin is

$$A_c = Ls \tag{4.18}$$

Substituting the values of perimeter and cross sectional area in the equation for m,

$$m = \sqrt{\frac{2h}{k_f s}} \tag{4.19}$$

From equation 4.2

$$d = \frac{4ab}{2(a+b)}$$

The channel hydraulic diameter can also be written as

$$d = \frac{2b}{1+\alpha} \tag{4.20}$$

And heat transfer coefficient h can be written as

$$h = \frac{Nuk(1+\alpha)}{2b} \tag{4.21}$$

Substituting the value of h in the equation for m

$$m = \sqrt{\frac{Nuk(1+\alpha)}{k_f s}} \tag{4.22}$$

The fin efficiency is given by

$$\eta = \frac{\tanh\left(\sqrt{Nu(1+\alpha)\beta\frac{k}{k_f}}\right)}{\sqrt{Nu(1+\alpha)\beta\frac{k}{k_f}}} \tag{4.23}$$

This result is particularly useful to determine the fin thickness required to achieve certain fin efficiency for given channel dimensions. Figure 4-3 shows the plot of channel aspect ratio versus the fin aspect ratio for various fin efficiencies. The results are obtained from equation 4.23. The analysis is useful when the channel dimensions are fixed and the thickness of fin is unknown. From the plot, for particular channel dimension and fin efficiency, the fin thickness can be easily found out.

For example, a channel aspect ratio of 4 and a desired fin efficiency of 0.9, β is 9.

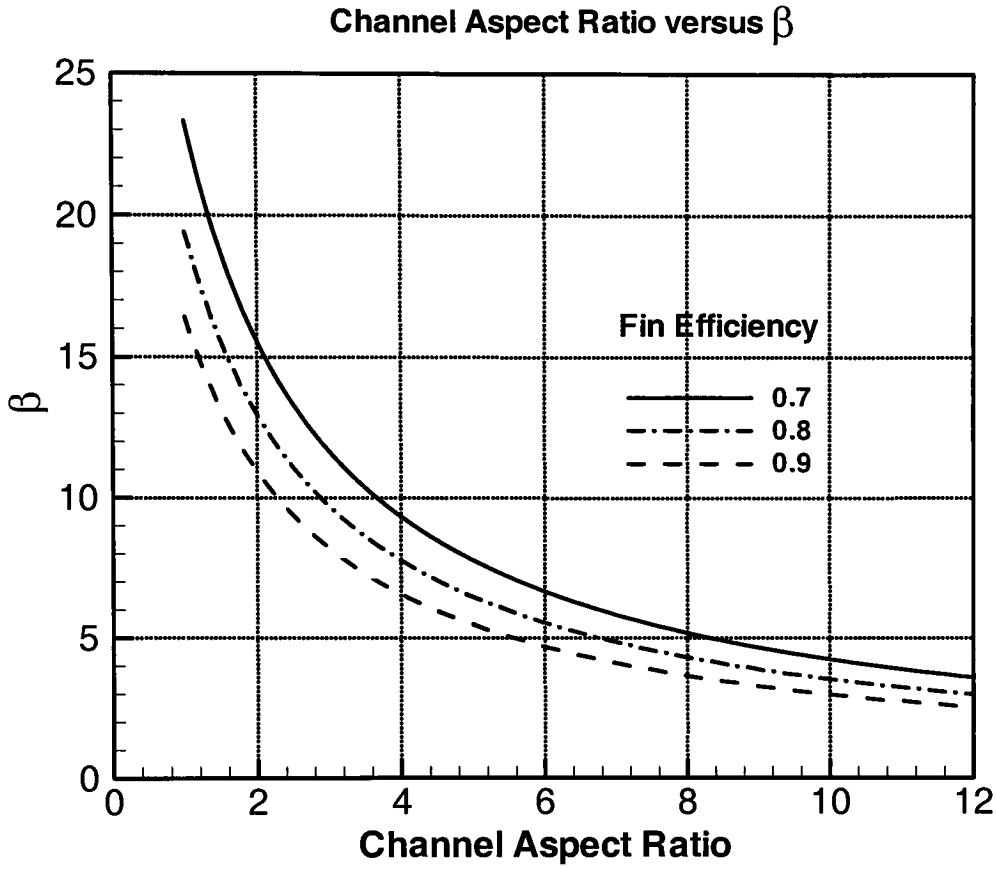

Figure 4-3: Fin Efficiency as a function of channel aspect ratio and β

4.5: Development of Heat Transfer and Pressure Drop Analysis Models

Cooling of a chip with active surface area of 10mm x 10mm is considered in the analysis. The channel width a and the fin thickness s are the parameters of interest. Initially the analysis is done assuming that the flow is hydrodynamically and thermally fully developed. The analysis is then extended to thermally developing flow and finally simultaneously developing flow is considered.

4.6: Assumptions

For the current analysis the following major assumptions are made –

1. Constant Heat Flux on the channel walls – Constant wall heat flux, with circumferentially constant wall temperature and axially constant wall heat flux is assumed. The heat flux along the length of the channel is constant, and the wall temperature varies along the channel length.

2. Heat losses from the cover plate are neglected – The cover plate on the microchannels is assumed to be insulated and hence the fin tip can be considered to be under adiabatic tip boundary condition. Although some heat will be conducted by the cover plate, it will be finally convected away by the fluid. By neglecting this heat transfer the solution will be on the conservative side.

3. The coolant flow is steady and incompressible. Since the fluid is pressured to only a few atmospheres at the inlet, incompressible flow is a valid assumption. The system is assumed to have a large sized reservoir on the inlet side which would guarantee a steady flow.

4. Uniform heat generation in the chip active area is assumed with no local hotspots. The heat generated is also assumed to constant temporally.

5. Constant properties are assumed for both the cooling fluid, water and wall material, silicon. (For water, k=0.61 W/mK, Cp=4180 J/kgK, Pr = 5.9, ρ=996 kg/m^3, $\nu = 8\times10^{-7}$ m^2/s at 300K, atmospheric pressure. Silicon, k=142 W/mK at 300K. Data obtained from National Institute of Science and Technology. www.nist.gov)

4.7: Types of Laminar Flows in Channels

Laminar flows in channels can be classified as fully developed flow, hydrodynamically developing, thermally developing and simultaneously developing flow. Figure 4-4 describes these flows for a fluid entering with uniform velocity and temperature.

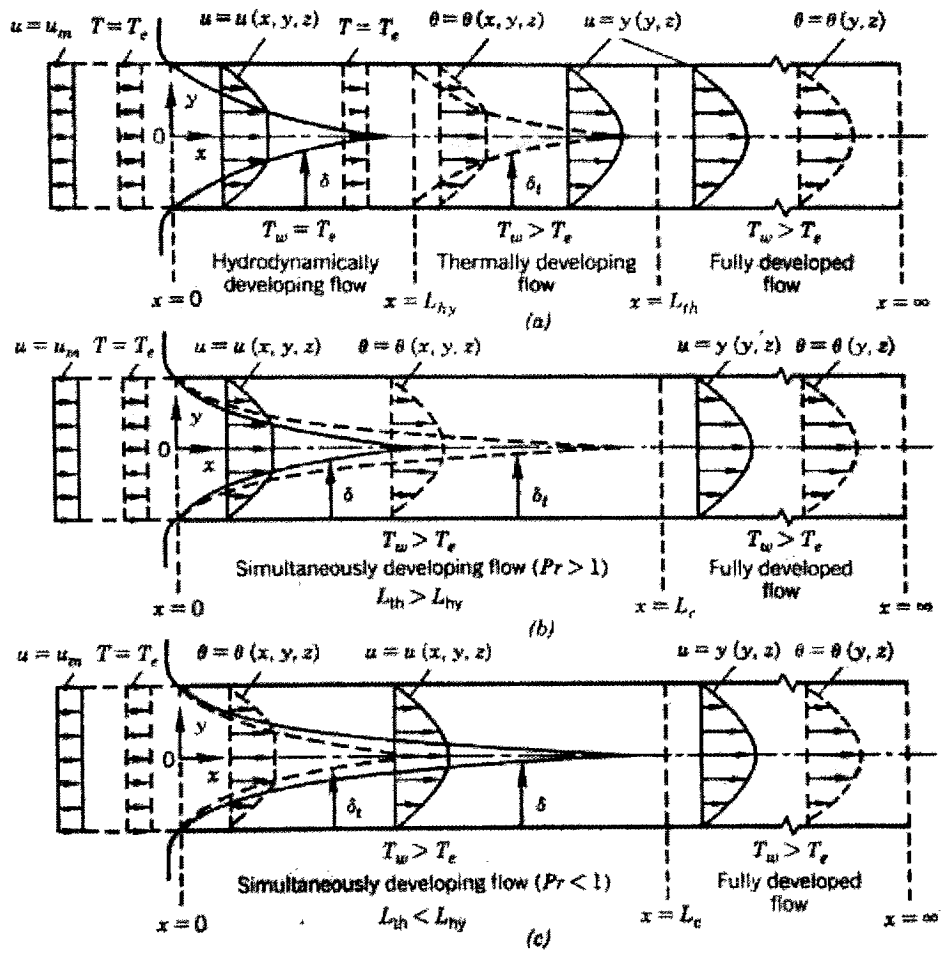

Figure 4-4: Types of Laminar Duct Flows for a constant wall temperature boundary condition. (a) Hydrodynamically developing flow followed by thermally developing and hydrodynamically developed flow (b) simultaneously developing flow, Pr>1 (c) simultaneously developing flow, Pr<1. Solid lines indicate velocity profiles and dashed lines indicate temperature profiles. (From Kakac *et al.*)

In Fig 4-4a, assume that the flow is isothermal till $x = L_{hy}$. The effect of viscosity spreads across the duct cross section starting from the entrance (x = 0). The hydrodynamic boundary layer δ varies as the axial distance x. The hydrodynamic boundary layer separates the flow into two regions – a viscous region near the walls and an inviscid region near the axis of the duct. In the viscous region the fluid motion is affected by the wall whereas the effect of wall is not affecting the fluid motion away from the wall. At L_{hy} the viscous effects have spread across the duct and the region $0 \le x \le L_{hy}$ is called the hydrodynamic entry length. Beyond $x = L_{hy}$, the axial velocity profile becomes independent of the axial coordinate.

After $x = L_{hy}$ let's consider that the channel wall is at a temperature greater than the inlet temperature. The thermal effects diffuse from the wall commencing at $x = L_{hy}$. The boundary layer thickness δ_t varies with the axial distance x. According to Prandtl's boundary-layer theory, the thermal boundary layer thickness divides the flow field into two regions, a heat affected region near the wall and an unaffected region around duct axis. At $x = L_{th}$, the thermal effects have completely spread across the duct section. The region $L_{hy} \le x \le L_{th}$ is termed as thermal entrance length. The region beyond L_{th} is fully developed flow. Figures 4-4b and 4-4c show simultaneously developing flow for Pr>1 and Pr<1 respectively.

4.8: Case A – Microchannel analysis assuming fully developed flow

For a fully developed flow with constant wall heat flux condition, the channel wall heat flux is given by

$$q'' = \frac{Q}{A_w} \tag{4.24}$$

Where Q is the heat load and A_w is the channel wall area. The channel wall area is

$$A_w = (2\eta_f b + a)Ln \tag{4-25}$$

The Nusselt number for a constant wall heat flux condition from Kakac *et al.* (1987) is

$$Nu = 8.235(1 - 2.0421\alpha + 3.0853\alpha^2 - 2.4765\alpha^3 + 1.0578\alpha^4 - 0.1861\alpha^5) \tag{4-26}$$

From the above equation, for a given α Nusselt number can be found out. From Eq. 4.4 the value of the convective heat transfer coefficient h is obtained. The maximum allowable surface temperature of the chip is a constraint. The maximum temperature on the chip will be at the exit. This surface temperature has to be below a certain threshold. The outlet temperature of the fluid can be given by

$$T_{out} = T_s - \frac{q''}{h} \tag{4-27}$$

The value of T_s is known before hand and the values of q'' and h are calculated considering the geometry of the channels. Once the outlet temperature, T_{out} is known, the mass flow rate required can be calculated by

$$\dot{m} = \frac{Q}{C_p(T_{out} - T_{in})} \tag{4-28}$$

The mass flow rate per channel $\dot{m}_c$ is found by dividing the total mass flow rate $\dot{m}$ by the number of channels. The velocity of fluid through each channel is

$$V = \frac{\dot{m}_c}{\rho ab} \tag{4-29}$$

where ρ is the density of the cooling fluid. The Reynolds number for the flow is

$$\mathrm{Re} = \frac{Vd}{\nu} \tag{4-30}$$

The pressure drop across the channels is given by the following equation

$$\Delta p = \frac{4(f\,\mathrm{Re})\mu VL}{2d^2} \tag{4-31}$$

where

$$C = f\,\mathrm{Re} \tag{4-32}$$

The value of C from Kakac *et al.* (1987) is

$$C = 24\left(1 - 1.3553\alpha + 1.9467\alpha^2 - 1.7012\alpha^3 + 0.9564\alpha^4 - 0.2537\alpha^5\right) \tag{4-33}$$

4.9: Case B – Microchannel analysis assuming developing flow

In case of the developing flow, the analysis is done in a different manner. The Nusselt number and the *fRe* correlation are not valid in the developing region. The data is available in the form of tabular data and graphs for Nu and $f_{app}Re$ respectively. Also the data is not only a function of channel aspect ratio α, but is also a function of the length from the entrance of the channel. For the hydrodynamically developing flow, the dimensionless axial distance x^+ is defined as

$$x^+ = \frac{x/d}{\mathrm{Re}} \tag{4-34}$$

The hydraulic entrance length is defined as the axial distance required to attain 99% of the ultimate fully developed maximum velocity when the entering flow is uniform. $f_{app}Re$ is a function of this hydrodynamic entry length x^+.

For thermal entrance region, the dimensionless distance x^* is defined as

$$x^* = \frac{x/d}{\mathrm{Re}\,\mathrm{Pr}} \tag{4-35}$$

The thermal entrance length is defined as the axial distance required to achieve a local Nusselt number is which is 1.05 times the fully developed Nusselt number value. Several investigators have studied laminar developing flow in rectangular channels. Apparent friction factors from Curr *et al.* (1972) $f_{app}\,\mathrm{Re}$ is presented in fig 4-5 as a function of x^+ and channel aspect ratio α. The data is presented in form of a graph in which four aspect ratios – 0, 0.2, 0.5 and 1 are plotted.

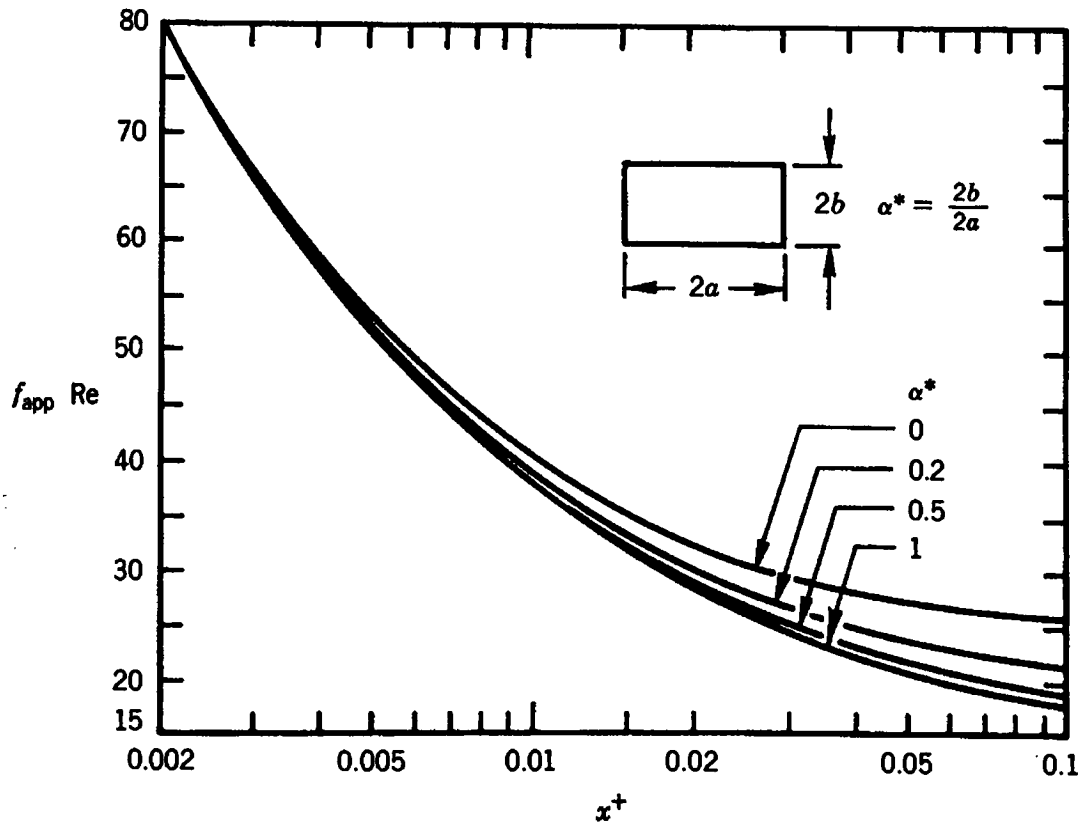

Figure 4-5: Apparent Friction factors for hydrodynamically developing flow in rectangular ducts.

For other values of α data is linearly interpolated. The pressure drop is given by

$$\Delta p = \frac{4(f_{app}\,\mathrm{Re})\mu V x}{2d^2} \tag{4-36}$$

Local Nusselt number for thermally developing flow is obtained from P. Wibulswas (1966). The data is presented in a tabular form for various values of x^* and channel aspect ratios α. Table 4-1 presents the local Nusselt numbers in the thermal entrance region of rectangular ducts. For a aspect ratio of zero (α =0), the channel geometry reduces to one of flow through parallel plates. Therefore for an aspect ratio of zero, the Nusselt number is calculated assuming flow through parallel plates. The data for Nusselt number for flat duct is obtained from Shah and London (1978).

In the developing flow analysis, to bring the axial distance from the entrance of the channel into the analysis, the channel length is divided into equal number of parts. The fRe and Nu is calculated for each division and the distance between the centre of the division and the entrance of the channel is used to calculate x^+ and x^*. So, for every division, the pressure drop and the heat transferred to the fluid is calculated. Also the surface temperature at that division is also computed. Since the heat to be dissipated is known, the heat load per channel per division can also be calculated knowing the number of channels and the number of divisions. Knowing the heat input for each division the bulk fluid temperature and the surface temperature of the chip at that particular division can be known. Detailed algorithm is presented in following section. The procedure can also be implemented without dividing the length. The divisions along the channel length are useful in case property change effects are to be considered or in case of a varying heat flux boundary condition.

The data that is presented in the form of a chart and a table is used in program. For this purpose, a curve fitting is done on the data. The curve fitting helps to eliminate the look up table and the lengthy code required to read values from the look up table. A one phase exponential decay type of curve fitting is employed for both, $f_{app}Re$ and Nu. The general expression for such a fit is given by

Y=Span*exp(-KX) + Plateau (4-37)

$\frac{1}{x^*}$	$\alpha = 1.0$	$\alpha = 0.5$	$\alpha = 1/3$	$\alpha = 0.25$
0	3.60	4.11	4.77	5.35
10	3.71	4.22	4.85	5.45
20	3.91	4.38	5.00	5.62
30	4.18	4.61	5.17	5.77
40	4.45	4.84	5.39	5.87
60	4.91	5.28	5.82	6.26
80	5.33	5.70	6.21	6.63
100	5.69	6.05	6.57	7.00
120	6.02	6.37	6.92	7.32
140	6.32	6.68	7.22	7.63
160	6.60	6.96	7.50	7.92
180	6.86	7.23	7.76	8.18
200	7.10	7.46	8.02	8.44

Table 4-1: Local Nusselt numbers in the thermal entrance region of Rectangular ducts.

The fit is done for each aspect ratio. For channel aspect ratio's in-between, the Nu and fRe values for the two closest known aspect ratio's is calculated and then linearly interpolated for the required aspect ratio. The equations are presented in a tabular form in table 4-2 and table 4-3

	$\alpha = 0$	$\alpha = 0.2$	$\alpha = 0.5$	$\alpha = 1$
Span	69.95	72.32	73.55	73.63
K	180.8	167.2	162.2	156.7
Plateau	27.54	23.85	22	20.82
R^2	0.9851	0.9814	0.9791	0.9765

Table 4-2: Best fit values for $f_{app}Re$ data.

	$\alpha = 0.25$	$\alpha = 0.3$	$\alpha = 0.5$	$\alpha = 1$
Span	-16.99	-9.536	-7.485	-6.521
K	0.001049	0.002215	0.003143	0.004066
Plateau	22.26	14.18	11.48	10.01
R^2	0.9982	0.9977	0.9984	0.9985

Table 4-3: Best fit values for Nu data

Knowing the values of x^+, x^* Nu_x and $f_{app}Re$ can be calculated from the equations developed. For a single division, we can write

$$T_{out} = \frac{Q_{div}}{\dot{m}_c C_p} + T_{in} \tag{4-38}$$

where Q_{div} is heat input per channel per division. This T_{out} is the T_{in} for the next division. The bulk temperature T_b for the division is the average of T_{in} and T_{out}. The surface temperature is calculated by

$$T_s = \frac{Q_{div}}{hA_{div}} + T_b \tag{4-39}$$

The T_s at the last division (at the exit where the surface temperature is maximum) should be less than the maximum allowable circuit temperature.

4.10 Algorithm for developing flow solution:

1. Certain number of channels is assumed at the start.
2. The ratio of fin thickness to channel width is assumed to be 1. Knowing the number of channels and F, the channel width and fin thickness can be found out.
3. The channel depth is fixed and is assumed to be known. The hydraulic diameter of the channel is calculated knowing the channel dimensions.
4. The channel length is divided into 'N' number of equal divisions. Since the thermal entry length and the hydraulic entry length are a function of axial distance from the entrance of the channels, the channel is divided into smaller divisions. The axial distance of each division from the channel entrance is the distance of the centre of that particular division from the entrance. This is shown in figure 4-6

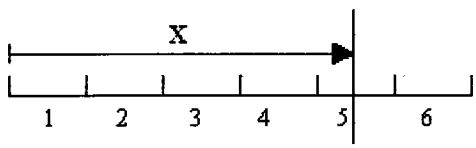

Figure 4-6: Channel divided into smaller number of parts along its length.

5. A small value of Reynolds number is assumed.
6. Knowing the Re, x^+ and x^* are calculated at the centre of each division. The curve fits developed are used to obtain the $f_{app}Re$ and Nu values at every section.
7. For every division, energy balance is applied and the outlet temperature of the coolant for that division is found out. This temperature is the inlet temperature

for the next division. The procedure is repeated till the last division and the surface temperature at the exit of the channel is compared with the maximum allowable circuit temperature. If the surface temperature at the exit is greater than the allowable circuit temperature, the Reynolds number is increased slightly and the entire procedure is repeated. The process is stopped once the outlet surface temperature is less than the maximum allowable chip temperature.

8. For a particular Re, the mass flow rate, pressure drop and pumping power required are found out.
9. The configuration which yields the minimum pressure drop out of the large range of possible configurations is the optimal configuration.

The analysis procedure can be used even in case of varying wall heat flux. In case of varying wall heat flux, the maximum chip surface temperature might not be at the exit. Such cases can be accommodated by making suitable changes in the code.

4.11 Heat Transfer Enhancement

Although the heat transfer coefficients are very high in case of microchannels, increase in heat dissipation rate is necessary to cool the chips further for dissipating heat loads in excess of $300W/cm^2$. To address this issue, an offset fin construction is utilized. In this type of construction, the fin instead of being 10 mm long (total length of the channel) is broken down into several smaller fins and also placed offset to each other. This concept is illustrated in figure 4-7.

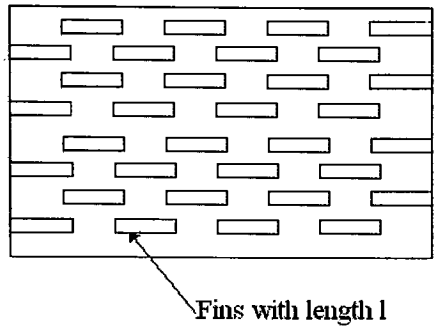

Figure 4-7: Offset Fins shown in the top view. The length of each fin is 'l'.

The analysis is carried out in a different manner to the earlier one. In this type of configurations, the fin length (i.e. length in the axial direction) is small and the heat transfer coefficient h and f_{app} Re are assumed to be constant over the entire length. The values of h and f_{app} Re are calculated in a similar fashion as explained previously, only difference being that the values are same for each fin. As a result a higher heat transfer coefficient is obtained but with the added penalty of a higher friction factor.

Another possible modification to the system is changing the flow pattern. Instead of pumping fluid from one side of the chip and taking it out from the other, a scheme in which fluid is pumped at the centre and taken out at both the ends is investigated. In this case, the pressure drop through the channels will be lower since the flow lengths are reduced. Also the heat transfer rate for the small passage length will be higher, which will result in a better performance.

Fully developed flow analysis is done for 100W and 200W heat load. Pressure drop plots are presented and the range of optimum channel configurations close to the optimum solution considering fully developed flow is identified. For the developing flow condition, a heat load of 200W is considered. Pressure drop and flow rate envelopes are plotted. From the plots a region of possible channel configurations is identified. A comparison between results obtained from fully developed flow analysis and developing flow analysis is done. The last section deals with the enhanced heat transfer analysis. Pressure drop and flow rate plots for an offset fin arrangement and with a split pass arrangement are presented.

5.1: Results for Case A: Fully developed flow assumption

Initially a fully developed flow is assumed and the analysis is carried out for constant wall heat flux boundary condition. A chip having an active surface area of 10mm X 10mm is considered. Pressure drop values are obtained for channels with varying depth and width. The fin thickness is assumed to a constant at 35 μm, which represents the minimum thickness that can be easily manufactured with current fabrication technology. Figure 5-1 shows the fin efficiency as a function of the fin thickness for a maximum fin height (channel depth) of 300 μm. A thick fin will have a better fin efficiency, but the number of channels decreases with an increase in the fin thickness, and the area available for heat transfer also decreases. With a fin thickness of 35 μm, the fin efficiency is above 90 percent. Although including fin thickness as a variable would lead to further refinements, the fabrication limit is believed to be the limiting factor.

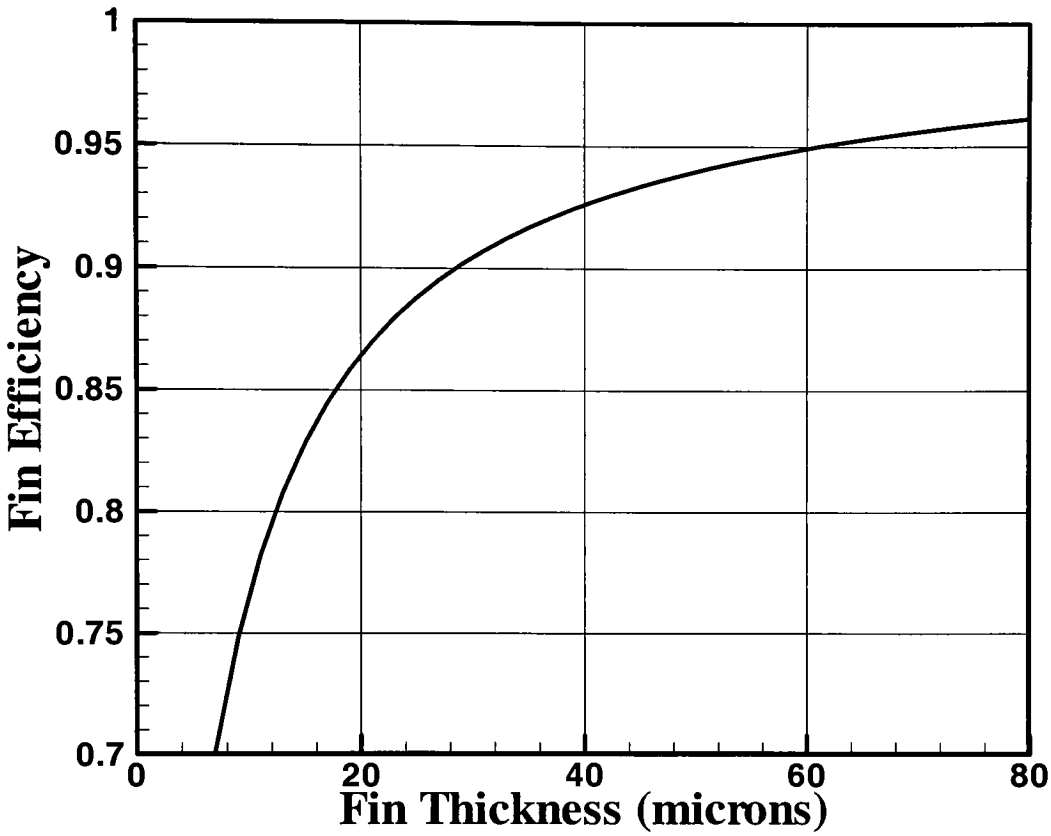

Figure 5-1: Fin efficiency for various fin thickness for a channel depth of 300μm.

The heat transfer coefficient h, for various channel dimensions can be calculated from Eq. 4-26. For a constant heat flux boundary condition, h values are shown in Fig. 5-2. The h values are very high as expected for microchannels. For channel depth of 50μm, at a small channel width (less than 100 μm), the h value decreases as the channel width increases. But after 100μm the h again increases. This is due to the fact that Nu increases as the channel gets skewed. Also the hydraulic diameter is changing as the channel width is changing. The figure 5-2 shows the combined effect of increasing hydraulic diameter and also the changing aspect ratio. Same is also true with other channel depths shown in the figure.

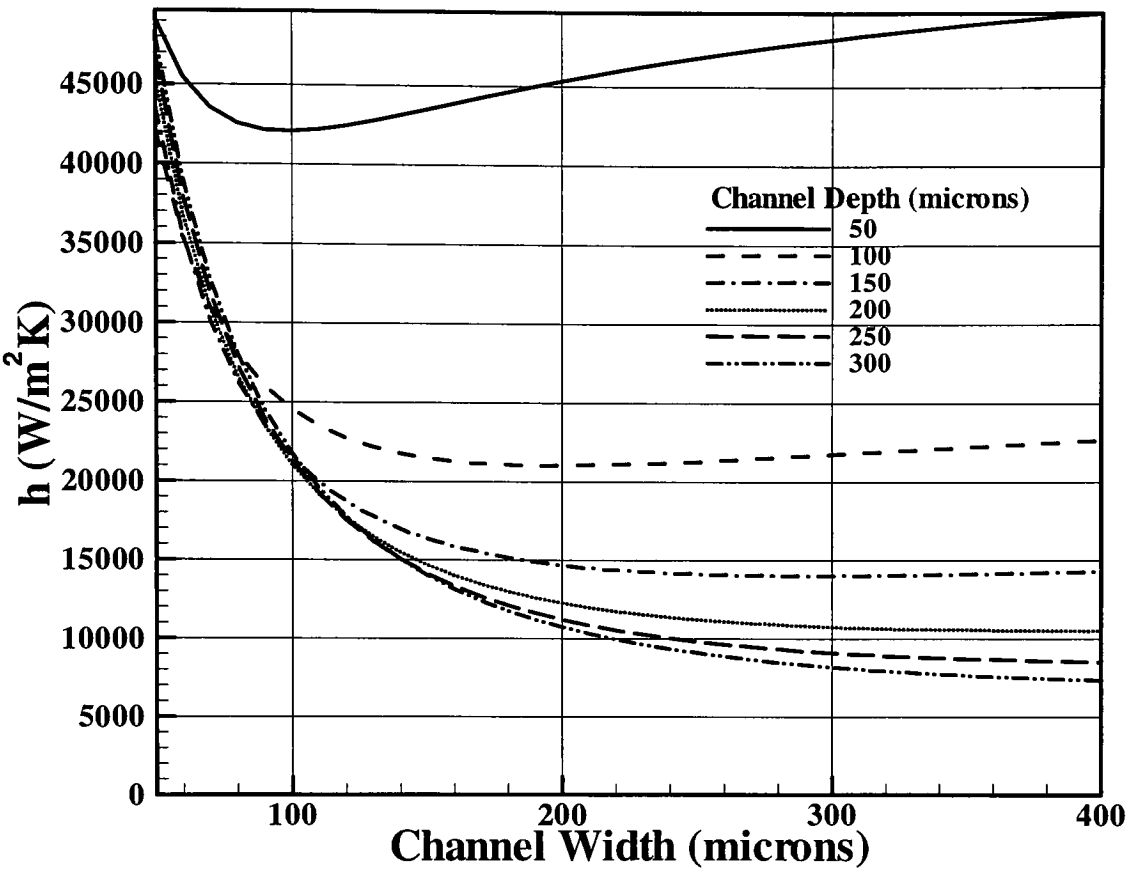

Figure 5-2: Variation of h with channel width for various channel depths assuming fully developed flow

The most important parameter is the pressure drop. The pressure drop plot for a heat load of 100 W on 10mm X 10mm chip is shown in figure5-3. As seen from the figure, the pressure drop for a very narrow channel is high, but the pressure drop decreases with increasing channel depth. As the channel width increases, the pressure drop decreases for any particular channel depth. Beyond a certain point, an increase in the width results in increase in pressure drop. This is due to the fact that as the width increases the number of channels that can be accommodated reduces. In this scenario, for the same heat load, the mass flow rate required through each channel increases thus increasing the pressure drop. This increase in mass flow rate is shown in figure 5-4. A judicious choice in this case will be a channel depth of 300μm and a channel width of 200μm. The pressure drop is minimum for this configuration and the flow rate required is also not too high. Flow rate increases drastically after 300μm channel width due to reasons discussed above.

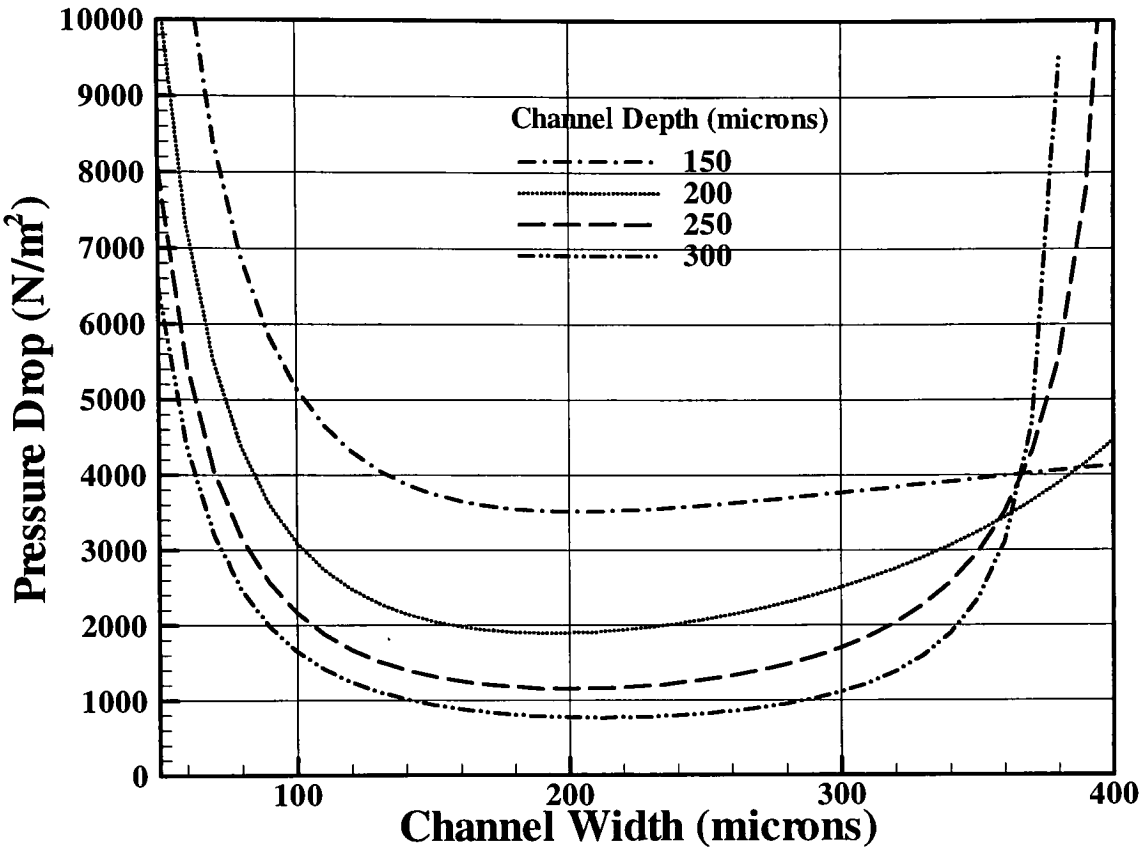

Figure 5-3: Pressure drop for a heat load of 100W assuming fully developed flow

Re also follows the trend shown in figure 5-4. The pumping power is very small and is not a main criterion for channel widths less than 300μm. Beyond 300μm the pressure drop and the flow rate, both increase dramatically increasing the pumping power requirement.

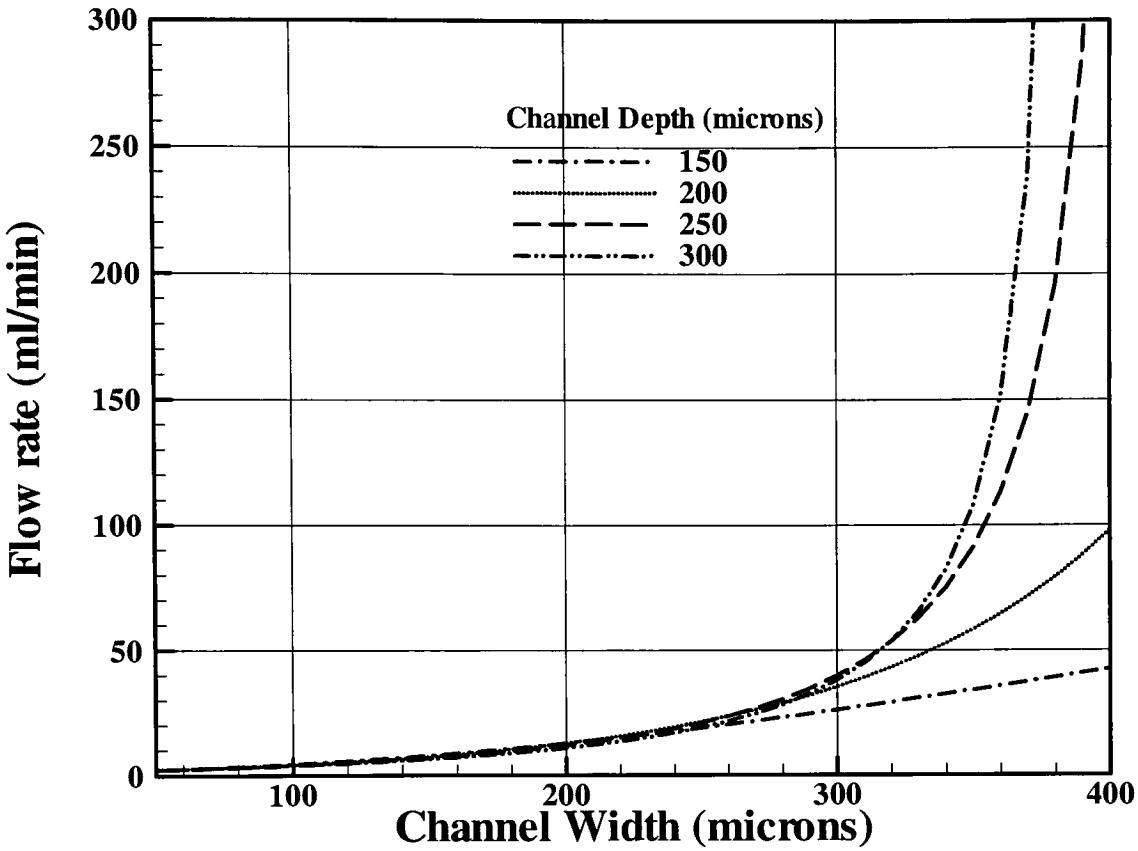

Figure 5-4: Flow rate for 100W heat load assuming fully developed flow

Similar plots are developed for designing a system for 200W heat load. Figure 5-5 shows plot for pressure drop when heat load is 200W. For 200W as expected the pressure drop is higher than for 100W case. In this case, the configuration for minimum pressure drop is a channel width of 140μm and a channel depth of 300μm. It is evident from the results that deeper channel is always better. But it should be noted that the fin efficiency goes down as the channel depth increases and although there is gain in hydraulic performance the gain in thermal performance is not substantial. Apart from this, increasing channel depth might require change in manufacturing process.

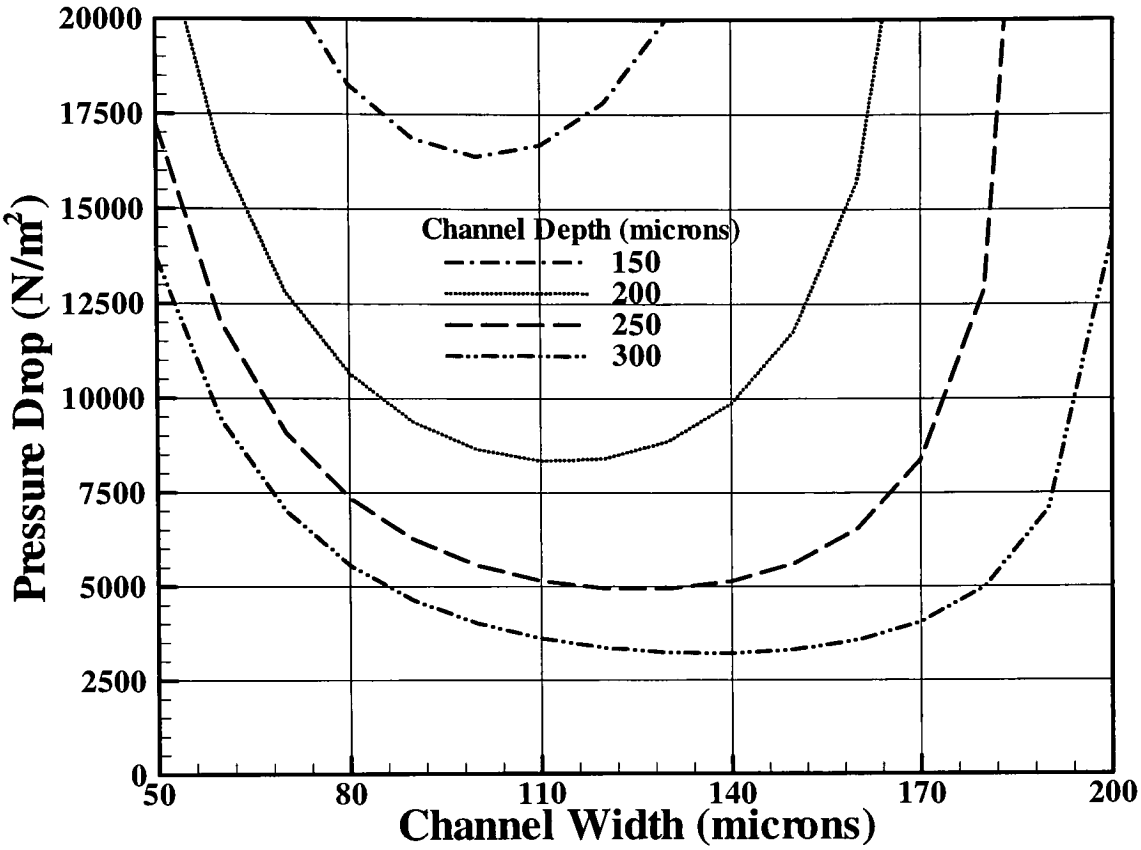

Figure 5-5: Pressure drop for a heat load of 200W assuming fully developed flow

5.2: Results for Case B: Developing flow assumption

For developing flow analysis a design envelope is developed with fin aspect ratio and channel number as the variables. A chip of 10mm X 10mm is considered and a heat load 200W is assumed. The channel depth is 200μm. The analysis is carried out for developing an envelope as discussed in chapter 4. The envelope is presented in the figure 5-6. The X axis represents number of channels and the Y axis represents the fin aspect ratio. The contour plot shows the pressure drop in kPa (dashed – dot lines). The solid lines indicate the fin thickness in μm. Since 30μm is the minimum thickness that can fabricated for a fin, the configurations represented by the area below 30μm are not feasible solutions. The channel number varies from 30 to 75. This range covers the minimum pressure drop region. Besides, with channel number less than 30 there are not

many feasible solutions due to 30μm fin thickness condition. For the region above 30μm line, a pressure drop of less than 9 kPa can be obtained for channel number in between 55 and 70. The fin aspect ratio should be in between 0.25 and 0.4. All the configurations in between these numbers will yield a lesser pressure drop than any other configurations. Once the fin aspect ratio and the number of channels are selected, the actual channel width and the fin thickness can be found out by equations 4.7 and 4.8.

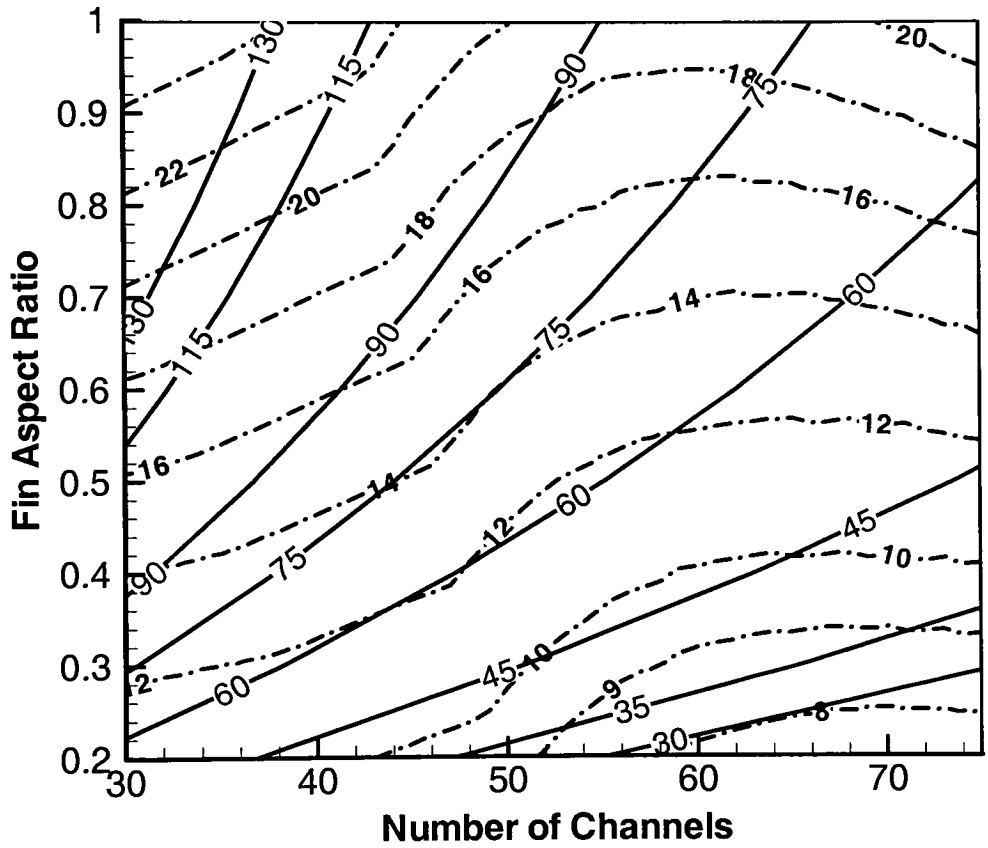

Figure 5-6: Contour plot showing Pressure Drop in kPa (dash dot lines). Solid lines indicate fin thickness (μm). Heat load is 200W

For example let us assume that we have decided to select 60 channels (n=60) and a fin aspect ratio of 0.3 (F=0.3) which yields a pressure drop of 8.8 kPa. Substituting these values in Eq 4.7 and Eq. 4.8 we get a channel width of 127μm and a fin thickness of

39μm. Contour plot for the flow rate is also developed and is shown in figure 5-7 for the same heat load and channel depth.

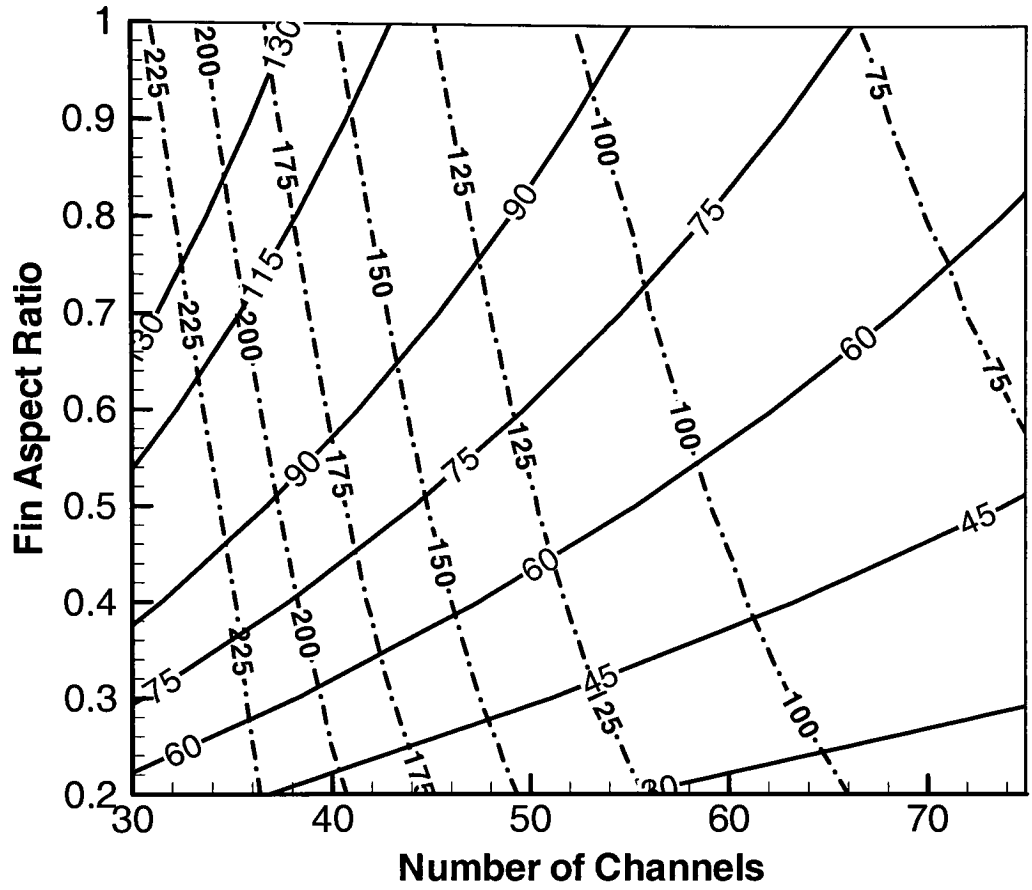

Figure 5-7: Contour plot showing Flow rate in ml/min (dash dot lines). Solid lines indicate fin thickness (μm). Heat load is 200W

The dash dot lines show contours for flow rate in ml/min. The solid lines indicate the fin thickness. For the design point considered earlier, the flow rate is 110 ml/min. The contour plot for pumping power is shown in figure 5-8. The plot shows contour lines for pumping power in mW.

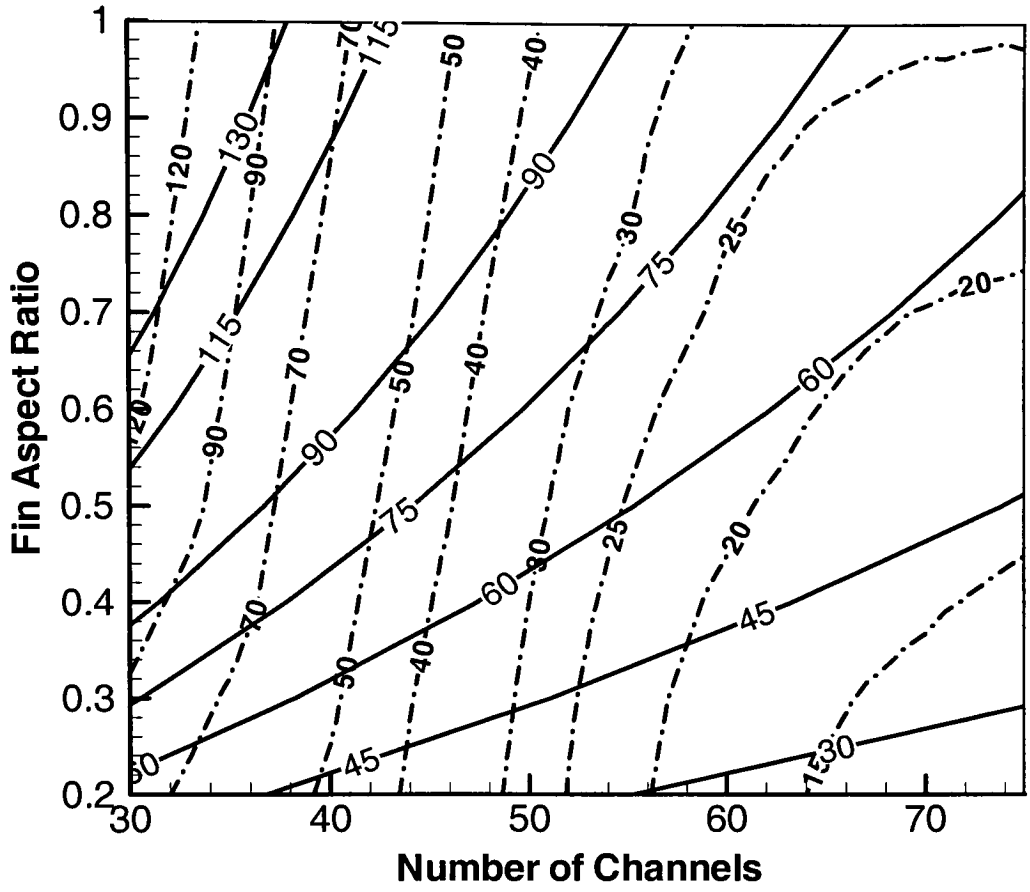

Figure 5-8: Contour plot showing Pumping Power in mW (dash dot lines). Solid lines indicate fin thickness (μm). Heat load is 200W

The pumping power plot closes the design problem completely as now we have all the information needed to fabricate the device which will satisfy all constraints with minimum pressure drop. Similar plots can be constructed for any other heat load or channel depth.

The 35μm fin thickness line is added to compare the results between fully developed flow and developing flow analysis. From figure 5-5, for 200μm channel depth, fully developed flow analysis results in optimum channel width of 110μm. Since the fin thickness is fixed to 35μm in the fully developed flow, using Eq. 4.8 the fin aspect ratio F

is 0.32 and the number of channels that can be fitted is 69. The pressure drop is 8.5 kPa. But with developing flow analysis the predicted pressure drop is higher. From the figure 5- 6 which shows contour plot for pressure when heat load is 200W an optimum solution can be obtained in between 55 to 74 channels and a fin aspect ratio of 0.25.

5.3: Comparison between fully developed and developing flow analysis

The fully developed flow analysis predicts a lower value of heat transfer coefficient. The thermally developing flow analysis predicts a higher Nusselt number in the entry region. For the range of Reynolds number under consideration, the entire channel length is in the thermally developing region. Friction factors are also higher during the developing region. For water, the Prandtl number is 5.9. In case of Pr>5, the velocity develops more rapidly than the temperature profile (from Kays and Crawford). A comparison is done between results obtained from both the methods

	Developed	**Developing**
Heat load (W)	200	200
Fin thickness (μm)	35	34.8
Channel width (μm)	110	116
Δp (kPa)	8	8.7

Table 5-3: Comparison between fully developed and developing flow analysis

5. 4: Enhanced Heat Transfer

For the enhanced heat transfer analysis, a 200μm x 200μm channel is considered with fin thickness of $100\mu m$. With this configuration, 33 channels can be constructed in a 10mm width.

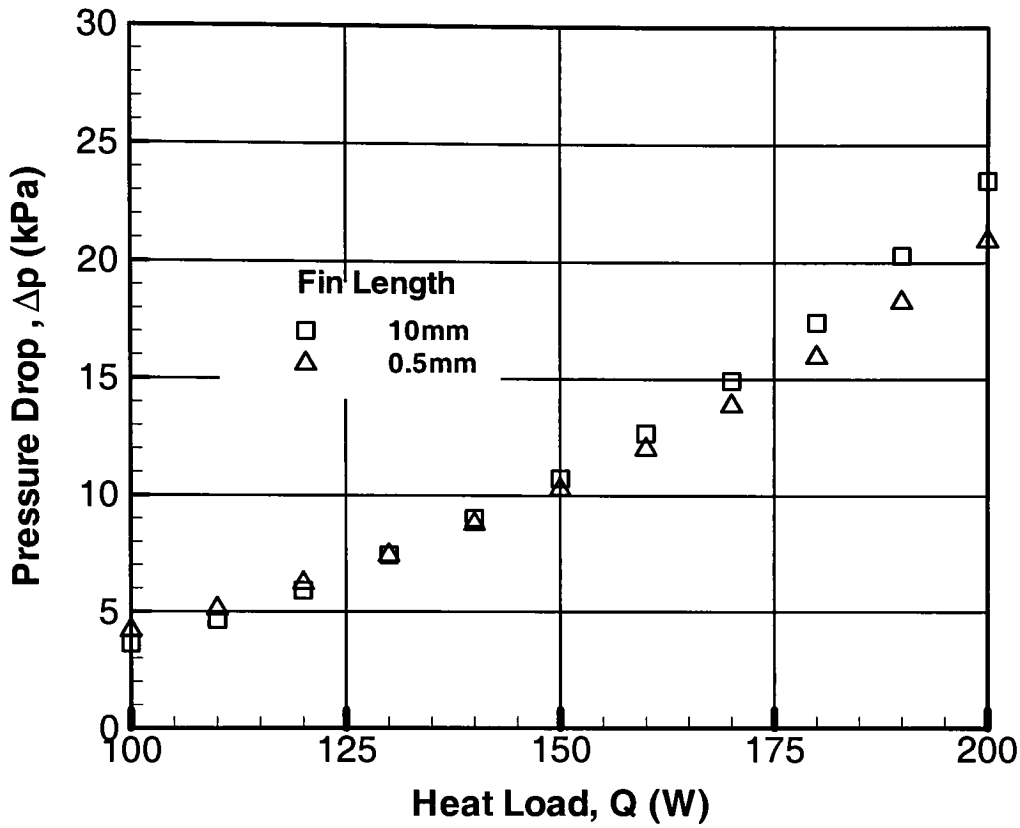

Figure 5-9: Heat load (W) versus Pressure Drop (kPa) for enhanced channels.

Figure 5-9 shows comparison between a single channel and enhanced channel with a fin length of 500μm. The pressure drop for enhanced channel is slightly lower than a single channel for same heat load. This is due to the fact that the heat transfer coefficient is very high in case of the enhanced channel geometry. Although a higher heat transfer rate is obtained for the same mass flow rate, the increase in friction factor counters the advantage gained. But the required flow rate is substantially reduced as seen from fig 5-10.

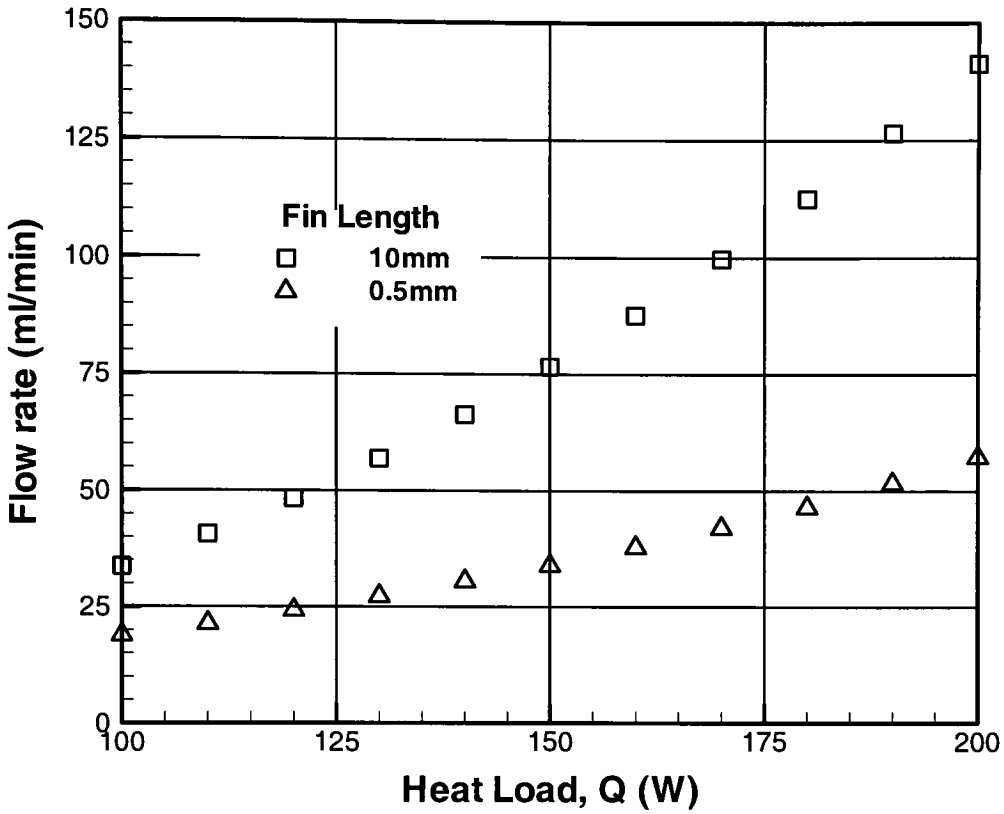

Figure 5-10: Heat load (W) versus Flow rate (ml/min) for enhanced channels.

The reductions in the flow rate and pressure drop reduce the pumping power requirement. In a two pass split arrangement, the pressure drop is reduced significantly. A similar design with a once through type of arrangement has a lower heat dissipation capacity for a given pressure drop limit. Figure 5-11 compares a once through arrangement to a two-pass split arrangement.

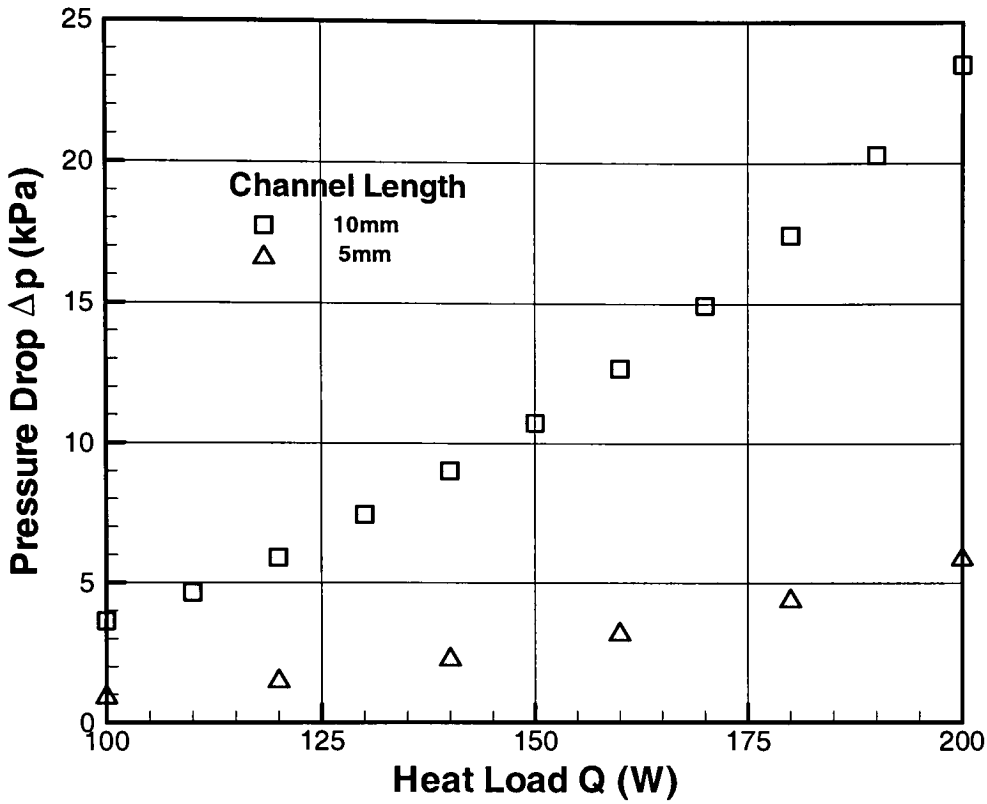

Figure 5-11: Comparison between single pass and two pass–split arrangements.

A two pass split arrangement is a definite improvement over a single pass configuration. The heat dissipation capacity for a specified pressure drop is almost twice that of a single pass arrangement. This improvement is a result of the increased heat transfer coefficient. Although the friction factor also increases, the reduced flow length helps in keeping the pressure drop low for a given heat dissipation rate. It must be noted that the entrance and exit losses are not calculated and can be a significant contributor the total pressure drop. The plot presents the pressure drop in the channels itself.

1. Direct liquid cooling of chips using microchannels offers a viable solution from a thermal and hydraulic viewpoint.

2. An analytical method has been developed for analyzing the thermohydraulic performance of microchannel flow geometry for direct chip cooling. The analysis is useful for laminar flow fully developed and developing flow conditions.

3. A relation between the channel aspect ratio and fin aspect ratio is developed. This relation is useful to determine the fin thickness required to achieve certain fin efficiency for given channel dimensions.

4. Pressure drop is a strong function of the channel geometry. Deeper channels are better. The channel width and fin thickness are very important parameters and must be selected judiciously.

5. A comparison between fully developed flow analysis and developing flow shows that the predicted pressure drop is slightly higher in case of developing flow analysis. A fully developed flow analysis is a quick way to come to a pressure drop estimate. But for a detailed analysis developing flow must be assumed.

6. For higher heat fluxes, plain microchannels require excessive water flow rates that impose severe pressure drop penalties. Providing enhanced offset split-fins with a split flow arrangement enables accommodating such high heat fluxes with a low core pressure drop.

7. Using the model that is presented, we can identify a region of possible channel configurations that will help in designing microchannels for direct chip cooling.

The current work only considers a chip of 10mm × 10mm. The methodology and equations presented here can be applied to other chip sizes in arriving at the desirable channel configurations.

Bergles, A.E., Linhard, J. H. V, Kendall, G.E., and Griffith, P., 2003, *Boiling and Condensation in Small Diameter Channels*, Heat Transfer Engineering, Vol 24 No1, pp 18-40.

Choquette, S.F., Faghri, M., Charmchi, M. and Asako, Y., 1996, Optimum design for microchannel heat sinks, 7th International Symposium on Information Storage and Processing Systems, Atlanta, Georgia, Nov 17-22, pp 115-126.

Curr,R.M., D. Sharma, and D.G. Tatchell, 1972, *Numerical Predictions of some Three Dimensional Boundary Layers in Ducts*, Computational Methods in Applied Mechanics and Engineering, Vol. 1, pp 143-158.

Garimella, S.V., and Singhal, V., 2004, *Single –Phase Flow and Heat Transport and Pumping Considerations in Microchannel Heat Sinks*, Heat Transfer Engineering, Vol. 25 No 1, pp 15-25.

Incropera, F.P., and DeWitt, D.P., 2002, *Fundamentals of Heat and Mass Transfer*, John Wiley & Sons, New York.

Kakac, S., Shah, R.K and Aung, W., 1987, *Handbook of Single-Phase Convective Heat Transfer*, John Wiley & Sons, New York.

Kays, W.M., and Crawford, M.E., 1993, *Convective Heat and Mass Transfer*, McGraw Hill, Inc.

Kim, S.J., 2004, *Methods for Thermal Optimization of Microchannel Heat Sinks*, Heat Transfer Engineering, Vol. 25 No 1, pp 37-49.

Knight, R.W., Goodling, J.S., and Hall, D.J., 1991, *Optimal Thermal Design of Forced Convection Heat Sinks – Analytical*, Journal of Electronic Packaging, September,1991, vol. 113 pp 313-321.

Knight, R.W., Hall, D.J., Goodling J.S., and Jaeger, R.C., 1992, *Heat Sink Optimization with Application to Microchannels*, IEEE Transactions on Components, Hybrids, and Manufacturing Technology, Vol. 15 No 5, pp 832-842.

Mudawar, I., and Qu, W., 2002, "Experimental and numerical study of pressure drop and heat transfer in a single-phase micro-channel heat sink", *Int. J. Heat and Mass Transfer,* Vol.45, pp.2549-2565.

Nakayama, Wataru, 1999, *Enhanced Heat Transfer in Tight Space – A Frontier for Thermal Management of Microelectronic Equipment, Enhanced Heat Transfer*, 1999, vol. 6, pp 121-133.

Phillips, R.J., 1987, *Forced Convection, Liquid Cooled, Microchannel Heat Sinks*, M.S. Thesis, Department of Mechanical Engineering, Massachusetts Institute of Technology.

Riddle, R.A., Contolini, R.J., and Bernhardt, A.F., 1991, *Design Calculation for the Microchannel Heat Sink*, National Electronic Packaging and Production Conference, NEPCON West '91, conference, February 24- 28, 1991, exposition, February 25-28, 1991, Anaheim Convention Center, Anaheim, California, pp 167-172.

Samalam, V.K., 1989, *Convective Heat Transfer in Microchannels*, Journal of Electronic Materials, Vol. 18 No 5, pp 611-617.

Sobhan, C.B., and Garimella, S.V., 2001, *A Comparative Analysis of Studies on Heat Transfer and Fluid Flow in Microchannels*, Microscale Thermophysical Engineering, Vol. 5 pp 293-311.